transient vagal reflex in one patient. These events occurred during DFPP, and fluid drip injection resulted in rapid recovery from these symptoms. A blood test revealed decreases in the hemoglobin as well as in the neutrophil and platelet counts; however, these were observed during IFN therapy, suggesting that they were unrelated to the DFPP. The ribavirin dose was reduced in three patients due to anorexia, anemia, and skin eruption. The IFN dose was reduced in one patient due to neutropenia. It was difficult to continue the IFN and ribavirin combination therapy in three patients due to skin eruption, anorexia, and systemic malaise; therefore, in these patients the therapy was discontinued.

4. Discussion

Currently, the most promising therapy for chronic hepatitis C is a 48-week PEG-IFN and ribavirin combination therapy. Using this approach, the SVR is increased in approximately 50% of patients [20]. However, in the other half, HCV viremia persists and, although ALT is stabilized, hepatitis activity may again increase several years later. Alternatively, chronic hepatitis persists without the normalization of ALT and may progress to liver cirrhosis resulting in hepatocellular carcinoma. To prevent these events from occurring, it is necessary to develop other novel ideas or novel drugs for therapy. With regard to ideas for therapy, long-term IFN therapy extended over 48 weeks, the use of intravenously administrable IFN-β, and concomitant IFN and high-dose ribavirin therapy with simultaneous monitoring of the blood ribavirin concentration, have been investigated [21]. With regard to novel drugs, amantadine, IL-12, and thymosin-α1 are concomitantly used with IFN therapy or with IFN and ribavirin combination therapy [22–24]. With regard to novel antiviral agents, the development of an antisense complex targeting the viral IRES, a serine protease inhibitor targeting NS3 protease, and a polymerase inhibitor targeting NS5B have been investigated [8–11].

Previous reports have described the various factors that affect the SVR produced by IFN therapy for chronic hepatitis. The patient-related factors include gender, age, the presence or absence of concomitant ribavirin treatment, and the stage of liver fibrosis; the viral factors include the viral genotype, HCV RNA level before therapy, and the number of mutations in the NS5A interferon sensitivity-determining region (ISDR) of genotype 1b [25]. Recently, an EVR has been recognized as an important factor for achieving an SVR using IFN therapy. An EVR is defined as virus elimination at an early stage after the initiation of treatment. An EVR in 2 weeks with IFN monotherapy and 12 weeks with IFNα-2b and ribavirin combination therapy has been shown to be frequent in SVR cases, and the probability of achieving an SVR is high when the virus is eliminated from the circulation within these early stages [12,13].

In this study, we focused on the HCV RNA level before therapy and attempted to reduce the viral load of chronic genotype 1b hepatitis C patients, with a high viral load of 100 KIU/ml or higher, by performing plasmapheresis therapy, DFPP, before the initiation of IFN therapy. Thus far, this is the first attempt to study the efficacy of a combination of IFN therapy and plasmapheresis with chronic hepatitis C patients.

In previous studies, Manzin et al. measured the HCV RNA in chronic hepatitis C patients with cryoglobulinemia before and after plasma exchange; they found that the HCV RNA was reduced by 45.3–93.3% after treatment but returned to its previous level after 4–6 h [14]. Similarly, Ramratnam et al. observed a decrease in the viral load after plasmapheresis in HIV-1- and HCV-positive patients [26]. It has also been reported that heparin-induced extracorporeal low-density lipoprotein (LDL) precipitation (HELP) apheresis decreased the HCV RNA in chronic hepatitis C patients with the complication of hypercholesterolemia [16,17,27]. The decrease in the HCV RNA was transient according to these reports. By fitting a mathematical model to the changes in viral load during IFN therapy, HCV production in the liver has been estimated to be 10^{12} particles per day [28]. Although the virus is eliminated from the blood, virus production continues in the liver unless it is inhibited by IFN; hence, the HCV RNA level may return to the pre-therapy level after a few hours. Therefore, we planned to administer IFN immediately after the first plasmapheresis.

We selected DFPP as a plasmapheresis technique because there was no necessity to exchange plasma and supplement albumin during the apheresis.

Since DFPP is based on the principle of size separation, the membrane with a mean pore size of 30 nm that was used as the second filter in this study can theoretically be expected to eliminate HCV particles with a diameter of 55–65 nm. After the DFPP second filtration, the HCV RNA was quantitatively undetectable after performing DFPP for 1 and 3 h; this implies that the filter could eliminate HCV particles and that the efficiency did not change with time.

Other low molecular weight substances, including albumin (MW 66 kDa) and ribavirin (MW 244 kDa), passed through the second membrane and were returned to patient's blood. Hence, low molecular weight substances were not eliminated by this DFPP system.

In seven patients, in whom the serum HCV RNA level could be measured before and after DFPP on day 1, the mean rate at which the HCV RNA level decreased was 48% (18–78%); the HCV RNA level did not increase again. This exclusion may have been due to the inhibition of virus production by the IFN therapy that was initiated immediately after DFPP.

The EVR after 2 weeks of therapy tended to be higher in the DFPP group than in the control group. The change in viral load after 2 weeks also tended to decrease more in the DFPP group than in the control group. However, both these differences were statistically insignificant. The virus negativity in the DFPP group after 4 and 8 weeks was 66.7% and 62.5%, respectively. In the control group, the HCV RNA levels were not measured periodically and therefore no comparison was

possible. However, in a double-blind, controlled study in Japan on IFNα-2b and ribavirin combination therapy for chronic genotype 1b hepatitis C patients with a high viral load, Iino et al. found that the HCV RNA negativity after 4 and 8 weeks after the initiation of therapy was 18.8% and 38.2%, respectively. This suggested that IFN therapy with a concomitant reduction of the viral load using DFPP may induce an early conversion to the HCV RNA-negative state.

In our study, an SVR was observed in 2 of the 9 patients (22.2%) in the DFPP group and in 2 of the 11 patients (18.2%) in the control group. These rates are comparable to the result in which an SVR was observed in 19.0% of chronic genotype 1b HCV patients after 24 weeks after the administration of an interferon and ribavirin combination therapy [30]. An SVR observed in DFPP group was not higher than that in control group although an EVR on 2 weeks in DFPP was relatively higher than that in control group. One of the possible reasons for this observation is that, in two of the six patients exhibiting an EVR, treatment was discontinued because of the adverse events. EVR was demonstrated to be the only factor related to SVR by univariate analysis in our study; this may have been because the number of patients was insufficient to conduct an accurate analysis of these factors.

With regard to the safety of the IFN and ribavirin combination therapy with concomitant DFPP, only mild hypotension and transient vagal reflex were observed after the initiation of DFPP, and these were rapidly resolved. There were no other adverse events attributable to concomitant DFPP, and the treatment was performed safely. Since DFPP is frequently used in the treatment of severe disease conditions, such as malignant rheumatoid arthritis, thrombotic thrombopenic purpura, and multiple sclerosis, there may be no problems with the application of this procedure to chronic hepatitis patients. During the treatment, a catheter was inserted in the right femoral vein for DFPP; however, no infection or accident occurred as a consequence of its indwelling. The other adverse events were attributable to the ribavirin and IFN therapy.

With regard to results of the blood test, the platelet count and fibrinogen level slowly decreased from the initiation of therapy until the completion of DFPP; however, these gradually recovered after the completion of DFPP. On day 3, the fibrinogen level was lower than 100 mg/dl in all but two patients. To ensure the safety of the patients, and to prevent complications such as hemorrhage, DFPP conducted three times on days 1, 2, and 4 during the first week of therapy may be appropriate for patients with chronic hepatitis C.

In view of the fact that we found no significant difference in the EVR and SVR between the DFPP and control groups, and because the number of patients was very small, it was not possible in this preliminary study to draw conclusions regarding the applicability of the DFPP used in conjunction with ribavirin and IFN therapy. It could be argued that a simple physical reduction in the viral load, induced by concomitant DFPP or other apheresis, is really significant for the ribavirin and IFN therapy for chronic hepatitis C patients with a high viral load. Based on our results, it may be possible to use DFPP to facilitate early viral elimination. However, the early viral elimination by DFPP was not related to an SVR. Although five of the eight patients (62.5%, therapy was discontinued in one patient after 7 weeks) became virus-negative after 8 weeks, an SVR was observed in only two patients; thus, the relationship between the early virus negativity obtained by DFPP and the SVR remains unclear. Since the early conversion to the virus-negative state is a result of the reactivity of the host and virus to ribavirin and IFN, it may be possible that a simple physical reduction in the amount of the virus is not significant. However, DFPP eliminates not only the virus but also macromolecules including immunoglobulins. The elimination of some humoral factors or complement components by the dialysis membrane might be involved. The state of HCV in the blood, such as the immunoglobulin-bound state, the lipoprotein-associated state, and the non-bound (free) state, may also be important. In two preliminary cases, the state of HCV during the treatment was investigated using differential flotation centrifugation. In differential floatation centrifugation, the hyperbaric fraction, including the immunoglobulin-bound HCV particles, settles to the bottom, whereas the hypobaric fraction, including free-state HCV particles, rises to the top. In the two examined cases, the bottom: top ratio was reduced after the first DFPP treatment; from 214 to 62 in case 1 and from 108 to 46 in case 2. Since a decline in the bottom: top ratio indicates an increased amount of free-state HCV particles compared to the amount of immunoglobulin-bound HCV particles, these results suggest that the occurrence of the free-state HCV increased after DFPP. This increase in the amount of free-state HCV may possibly involve an SVR; this supposition is based on a previous study that demonstrated that a high proportion of free-state HCV was related to an SVR [29].

In conclusion, in order to achieve a reduction in the level of HCV RNA before IFN therapy and to facilitate an early conversion to a virus-negative state, plasmapheresis therapy (DFPP) was performed on chronic genotype 1b hepatitis C patients with a high viral load. The therapy was performed without the occurrence of severe adverse events, and the results suggested the possibility that concomitant DFPP increased the rate of early conversion to a virus-negative state. Since only nine patients were treated and IFN administration was discontinued in three patients, the relationship between DFPP and an EVR or SVR is unclear. If an EVR is achieved by a combination of DFPP and interferon therapy, and this is related to an SVR, the combination therapy with DFPP will not only be of benefit to chronic hepatitis C patients with a high viral load but may also shorten the period of interferon therapy. Furthermore, the cost of interferon therapy will also be reduced, although the cost of performing DFPP three times will remain high at approximately 2500 dollars. Because our study was limited by the small number of patients, further investigations using a study design that clarifies the relationship between DFPP and an EVR or SVR are necessary. It is also important to further investigate the

antiviral effect of the PEG-IFN and ribavirin combination therapy with concomitant DFPP, and the effects of DFPP other than virus elimination. In order to clarify this relationship, a multi-center clinical trial is being undertaken in Japan, and the data from this study is currently being collected.

Acknowledgements

This study was supported by Asahi Kasei Medical Co. Ltd. (Tokyo, Japan). We thank Satoshi Saikawa, Hidetomo Takeuchi, and Tomoko Ino for providing technical support.

References

[1] Yoshida H, Shiratori Y, Moriyama M, et al. Interferon therapy reduces the risk for hepatocellular carcinoma: national surveillance program of cirrhotic and noncirrhotic patients with chronic hepatitis C in Japan. IHIT Study Group. Inhibition of hepatocarcinogenesis by interferon therapy. Ann Intern Med 1999;131:174–81.

[2] McHutchison JG, Gordon SC, Schiff ER, et al. Interferon alfa-2b alone or in combination with ribavirin as initial treatment for chronic hepatitis C. Hepatitis Interventional Therapy Group. N Engl J Med 1998;339:1485–92.

[3] Iino S, Matsushima T, Kumada H, Kiyosawa K, Kakumu S, Hayashi Y. Comparison of ribavirin (SCH18908) and interferon α-2b combination therapy and interferon α-2b monotherapy in chronic hepatitis C patients of genotype 1b and high viral load—a double blind parallel study to determine dosage and administration. Rinsyou Iyaku (J Clin Therap Med) 2002;18:565–91.

[4] Poynard T, Marcellin P, Lee SS, et al. Randomised trial of interferon alpha 2b plus ribavirin for 48 weeks or for 24 weeks versus interferon alpha 2b plus placebo for 48 weeks for treatment of chronic infection with hepatitis C virus. International Hepatitis Interventional Therapy Group (IHIT). Lancet 1998;352:1426–32.

[5] Poynard T, McHutchison J, Goodman Z, Ling MH, Albrecht J. Is an "a la carte" combination interferon alfa-2b plus ribavirin regimen possible for the first line treatment in patients with chronic hepatitis C? The ALGOVIRC Project Group. Hepatology 2000;31:211–8.

[6] Fried MW, Shiffman ML, Reddy KR, et al. Peginterferon alfa-2a plus ribavirin for chronic hepatitis C virus infection. N Engl J Med 2002;347:975–82.

[7] Iino SOK, Omata M, Kumada H, Hayashi N, Tanikawa K. Clinical efficacy of PEG-interferon α-2b and ribavirin combination with interferon α-2b and ribavirin combination therapy for 24 weeks. KAN TAN SUI 2004;49:1099–121 [in Japanese].

[8] Lamarre D, Anderson PC, Bailey M, et al. An NS3 protease inhibitor with antiviral effects in humans infected with hepatitis C virus. Nature 2003;426:186–9.

[9] Love RA, Parge HE, Yu X, et al. Crystallographic identification of a noncompetitive inhibitor binding site on the hepatitis C virus NS5B RNA polymerase enzyme. J Virol 2003;77:7575–81.

[10] Soler M, McHutchison JG, Kwoh TJ, Dorr FA, Pawlotsky JM. Virological effects of ISIS 14803, an antisense oligonucleotide inhibitor of hepatitis C virus (HCV) internal ribosome entry site (IRES), on HCV IRES in chronic hepatitis C patients and examination of the potential role of primary and secondary HCV resistance in the outcome of treatment. Antivir Ther 2004;9:953–68.

[11] Pudi R, Ramamurthy SS, Das S. A peptide derived from RNA recognition motif 2 of human 1a protein binds to hepatitis C virus internal ribosome entry site, prevents ribosomal assembly, and inhibits internal initiation of translation. J Virol 2005;79:9842–53.

[12] Davis GL. Monitoring of viral levels during therapy of hepatitis C. Hepatology 2002;36:S145–51.

[13] Davis GL, Wong JB, McHutchison JG, Manns MP, Harvey J, Albrecht J. Early virologic response to treatment with peginterferon alfa-2b plus ribavirin in patients with chronic hepatitis C. Hepatology 2003;38:645–52.

[14] Manzin A, Candela M, Solforosi L, Gabrielli A, Clementi M. Dynamics of hepatitis C viremia after plasma exchange. J Hepatol 1999;31:389–93.

[15] Fabrizi.F, Martin P, Dixit V, et al. Biological dynamics of viral load in hemodialysis patients with hepatitis C virus. Am J Kidney Dis 2000;35:122–9.

[16] Schettler V, Monazahian M, Wieland E, et al. Reduction of hepatitis C virus load by H.E. L. P.-LDL apheresis. Eur J Clin Invest 2001;31:154–5.

[17] Schettler V, Monazahian M, Wieland E, Thomssen R, Muller GA. Effect of heparin-induced extracorporeal low-density lipoprotein precipitation (HELP) apheresis on hepatitis C plasma virus load. Ther Apher 2001;5:384–6.

[18] Kaito M, Watanabe S, Tsukiyama-Kohara K, et al. Hepatitis C virus particle detected by immunoelectron microscopic study. J Gen Virol 1994;75:1755–60.

[19] Ichida F. New Inuyama classification: new criteria for histological assessment of chronic hepatitis. Int Hepatol Commun 1996;6:112.

[20] Saracco G, Olivero A, Ciancio A, Carenzi S, Rizzetto M. Therapy of chronic hepatitis C: a critical review. Curr Drug Targets Infect Disord 2003;3:25–32.

[21] Lindahl K, Stahle L, Bruchfeld A, Schvarcz R. High-dose ribavirin in combination with standard dose peginterferon for treatment of patients with chronic hepatitis C. Hepatology 2005;41:275–9.

[22] Abbas Z, Hamid SS, Tabassum S, Jafri W. Thymosin alpha 1 in combination with interferon alpha and ribavirin in chronic hepatitis C patients who are non-responders or relapsers to interferon alpha plus ribavirin. J Pak Med Assoc 2004;54:571–4.

[23] Poo JL, Sanchez-Avila F, Kershenobich D, Garcia-Samper X, Gongora J, Uribe M. Triple combination of thymalfasin, peginterferon alfa-2a and ribavirin in patients with chronic hepatitis C who have failed prior interferon and ribavirin treatment: 24-week interim results of a pilot study. J Gastroenterol Hepatol 2004;19:S79–81.

[24] Kullavanuaya P, Treeprasertsuk S, Thong-Ngam D, Chaermthai K, Gonlachanvit S, Suwanagool P. The combined treatment of interferon alpha-2a and thymosin alpha 1 for chronic hepatitis C: the 48 weeks end of treatment results. J Med Assoc Thai 2001;84(Suppl 1):S462–8.

[25] Pascu M, Martus P, Hohne M, et al. Sustained virological response in hepatitis C virus type 1b infected patients is predicted by the number of mutations within the NS5A-ISDR: a meta-analysis focused on geographical differences. Gut 2004;53:1345–51.

[26] Ramratnam B, Bonhoeffer S, Binley J, et al. Rapid production and clearance of HIV-1 and hepatitis C virus assessed by large volume plasma apheresis. Lancet 1999;354:1782–5.

[27] Marson P, Boschetto R, De Silvestro G, et al. Changes in HCV viremia following LDL apheresis in a HCV positive patient with familial hypercholesterolemia. Int J Artif Organs 1999;22:640–4.

[28] Neumann AU, Lam NP, Dahari H, et al. Hepatitis C viral dynamics in vivo and the antiviral efficacy of interferon-alpha therapy. Science 1998;282:103–7.

[29] Sakai A, Kaneko S, Matsushita E, Kobayashi K. Floating density of hepatitis C virus particles and response to interferon treatment. J Med Virol 1998;55:12–7.

[30] Nagaki M, Imose M, Naiki T, et al. Prospective study on early virologic response to treatment with interferon alpha-2b plus ribavirin in patients with chronic hepatitis C genotype 1b. Hepatol Res 2005;33:285–91.

J. Exp. Clin. Cancer Res., 25, 1, 2006

Analysis of Intrahepatic Lymphocyte Subsets in a Transgenic Mouse Model of Immune-Mediated Hepatocarcinogenesis

Y. Nakamoto and S. Kaneko

Department of Gastroenterology, Graduate School of Medicine, Kanazawa University, Kanazawa, - Japan

Long-term, persistent liver cell injury increases the risk for hepatocellular carcinoma (HCC) development in chronic viral hepatitis. In support of this notion, we have developed a unique animal model of chronic immune-mediated liver disease that induces hepatocellular carcinogenesis using HBV transgenic mice; however, the intrahepatic inflammatory response was not precisely evaluated. The current study demonstrated that hepatitis B surface antigen (HBsAg)-specific cytotoxic T lymphocytes (CTLs) were detected at a frequency of 0.05% of CD8+ T lymphocytes in the liver, and that monocytes/macrophages were remarkably increased as the disease developed. These results suggest that a minimal number of intrahepatic virus-specific CTLs and the recruited monocytes/macrophages may contribute to the process of chronic liver inflammation.

Key Words: Chronic hepatitis, Hepatocellular carcinoma, Intrahepatic lymphocytes, Transgenic mice

Almost all cases of hepatocellular carcinoma (HCC) occur after many years of chronic hepatitis due to a wide array of viral and nonviral etiologies in addition to hepatitis B and C viruses (HBV and HCV) (1,2). Chronic active hepatitis is characterized by indolent and progressive liver cell injury with associated hepatocellular regeneration (ie, cellular DNA synthesis) and inflammation (ie, the production of mutagens) which could, theoretically, precipitate random genetic and chromosomal damage and lead to the development of HCC (3).

In an effort to clarify the carcinogenic potential of chronic inflammation, we have developed a model of chronic immune-mediated liver disease using HBV transgenic mice that express the envelop proteins in the hepatocyte (4). The results demonstrate that continuous intrahepatic inflammation is sufficient to cause liver cancer in the absence of pre-existing viral transactivation, insertional mutagenesis or genotoxic chemicals during chronic HBV infection. Most importantly, a hepatitis B surface antigen (HBsAg)-specific cytotoxic T lymphocyte (CTL) response was detectable in the spleen of these animals, the strength of which corresponded with the number and size of their liver tumors. However, intrahepatic inflammation was not precisely evaluated in this model of HCC development. The current study was undertaken to determine the proportions of lymphocyte subsets in the livers of these animals that can display the high procarcinogenic potential in the process of chronic immune-mediated hepatitis.

The animal model of chronic hepatitis was generated using HBsAg transgenic mouse lineage 107-5D (official designation Tg[Alb-1,HBV]Bri66) (inbred B10D2, H-2d) kindly provided by Dr. F.V. Chisari (The Scripps Research Institute, La Jolla, California)(5), as described previously (4). Briefly, male HBsAg transgenic mice were thymectomized, irradiated (900 cGy), and their hemopoietic systems were reconstituted with bone marrow cells from syngeneic nontransgenic B10D2 (H-2^d) mice. One week after the bone marrow transfer, the animals received the $1x10^8$ splenocytes from nontransgenic B10D2 (H-2^d) mice that were infected intraperitoneally with a recombinant vaccinia virus expressing HBsAg (HBs-vac) 3 weeks before the splenocyte transfer (6). Serum alanine aminotransferase (ALT) activity increased in the recipients within 7 days after adoptive transfer, and fell progressively thereafter. Furthermore, serum ALT activity never returned to baseline in these animals, remaining at least 2-3 times above normal throughout the experiment.

To evaluate the intrahepatic lymphocyte subsets in the mice developing long-term, persistent hepatitis,

intrahepatic lymphocytes (IHLs) were isolated and stained with the following monoclonal antibodies (mAbs): anti-mouse CD4-fluorescein isothiocyanate (FITC) (RM4-5), anti-mouse CD8-phycoerythrin (PE), anti-mouse CD11b-FITC (M1/70), and anti-mouse CD19-PE (1D3) (BD PharMingen, San Diego, California). Cells were resuspended in PBS containing 2% formaldehyde, and analyzed on a FACSCalibur™ flow cytometer using CELLQuest™ software (Becton Dickinson, San Jose, California). The proportions of IHL subsets were indicated in Figure 1. Since the total numbers of isolated cells from the inflamed mice were 3.4 times of those from unmanipulated transgenic mice, cell numbers of all the subsets were increased as the disease developed (Figs. 1a and 1c). Among the subsets obtained from the inflamed mice, the percentages of $CD11b^+$ monocytes/macrophages were remarkably increased; $CD8^+$ T lymphocytes and $CD19^+$ B lymphocytes proportions were comparable; in contrast, $CD4^+$ cell proportions were decreased, in comparison with the unmanipulated mice.

Based on the results that the same transgenic mice developed an acute MHC class I-restricted necroinflammatory liver disease following the adoptive transfer of HBsAg-specific CTLs(5-7), we further estimated the frequencies of the HBsAg-specific CTLs by intracellular staining of IFNγ after the stimulation with the epitope peptide. Briefly, IHLs were cultured for 5 hrs at 37°C in complete RPMI medium containing 10% FBS in the presence or absence of 10^{-7} M of the peptide representing residues 28-39 (IPQSLDSWWTSL) of HBsAg that was identified as the epitope of the CTL in this model [Nakamoto, 1998 #26] or the lymphocytic choriomeningitis virus nucleoprotein (LCMV NP) peptide (PQASGVYML). Brefeldin A (Sigma, St. Louis, Missouri), which inhibits exocytosis of the cytokines, was added at a final concentration of 2 μg/ml. Subsequently, the cells were stained with Cy-Chrome-conjugated anti-mouse CD8 mAb (53-6.7) (BD PharMingen). They were then permeabilized using the Cytofix/Cytoperm kit (BD PharMingen) and stained with allophycocyanin (APC)-conjugated rat mAb specific for mouse IFNγ (XMG1.2) or its isotype control Ab (rat IgG1) (BD PharMingen). Cells were resuspended in PBS containing 2% formaldehyde, and analyzed on a flow cytometer (50,000-300,000 gated events acquired per sample).

As shown in Figure 1, HBsAg-specific $CD8^+$ CTL were analyzed by flow cytometry and detected in the upper-right quadrants (UR) on a dot plot of CD8 /

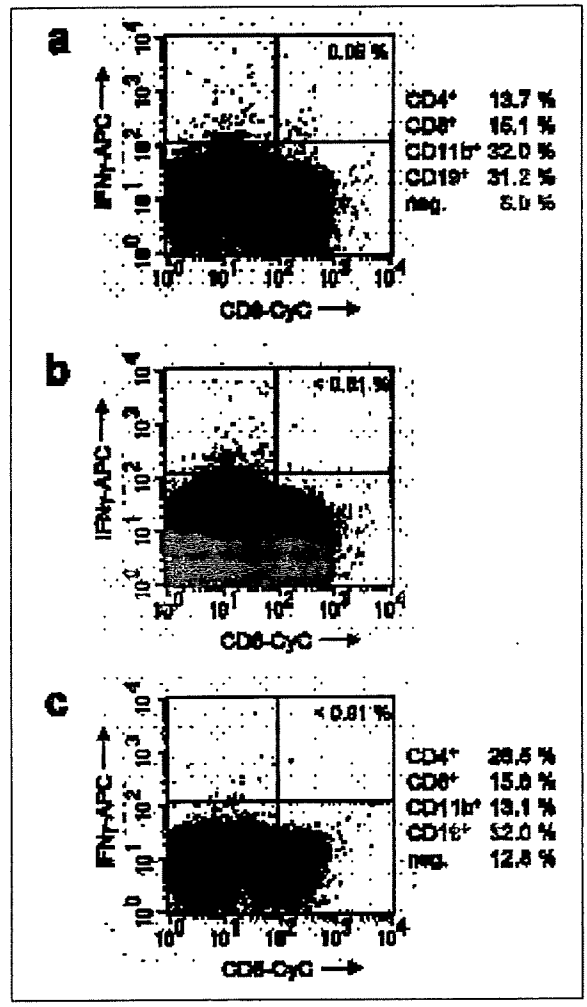

Fig. 1 - Quantitation of intrahepatic lymphocyte (IHL) subsets and detection of hepatitis B surface antigen (HBsAg)-specific CD8+ T lymphocytes in hepatitis B virus (HBV) transgenic mice. The transgenic mice were sacrificed 7 days after the splenocyte transfer, and IHLs were obtained (a and b). IHLs were also isolated from unmanipulated transgenic mice (c). The total numbers of isolated cells from the inflamed mice were 3.4 times of those from the unmanipulated mice. The percentages of CD4+, CD8+, CD11b+ and CD19+ cells were indicated in a and c. Otherwise, the obtained cells were cultured for 5 hr at 37 oC in the presence or absence of 10-7 M peptide representing residues 28-39 (IPQSLDSWWTSL) of HBsAg (a and c) or control LCMV NP (PQASGVYML) (b). After peptide incubation, the cells were analyzed for intracellular IFNg expression by flow cytometric analysis. The percentages indicated in the upper-right quadrants represent the proportions of intracellular IFNg+ cells of CD8+ T lymphocytes.

IFNγ. 0.05% of $CD8^+$ T lymphocytes were quantitated in IHLs from inflamed HBV transgenic mice (Fig. 1a), which were much less than those (~ 1%) reported in the CTL clone-induced, acute liver cell injury (7). The specificity of the CTL detection was confirmed by the stimulation with control LCMV NP peptide, in which the percentages of $IFN\gamma^+$ cells were less than 0.01% (Fig. 1b). In addition, the background level of the staining procedure after the peptide stimulation was less than 0.01% based on the results of IHLs isolated from unmanipulated transgenic mice (Fig. 1c). The frequencies of the CTL were confirmed by staining with the tetramer consisting of MHC class I (L^d) molecules and the epitope peptide (not shown). The cytotoxic activity of the CTL was detected after 2 weeks *in vitro* stimulation with the HBsAg (not shown). Moreover, although spleen cells, lymph node cells and PBMC were isolated from the inflamed mice and stained at the same time as IHLs, the $IFN\gamma^+$ cells were less than 0.01%, indicating that frequencies of the CTL are below the limit of detection in these organs but liver tissues. Collectively, the data demonstrate that a minimal number of intrahepatic antigen-specific CTLs may play an important role in the development of long-term, persistent liver disease.

Previous studies demonstrate that HBsAg-specific $CD8^+$ CTL clones cause an acute necroinflammatory liver disease in HBV transgenic mice (6,7). The acute hepatocellular injury terminates within 5 days after the CTL clone injection in contrast to the long-lasting inflammatory response in the current model. In our previous study on chronic liver disease, we did not define the cellular basis for the persistent hepatocellular injury (4). In the current study, antigen-specific $CD8^+$ CTLs were detected in the liver tissues, suggesting to contribute to the development of prolonged chronic hepatitis. This may be consistent with our observations that $CD8^+$ subset depletion reduced the peak of hepatocellular injury and the persistence of liver disease, while the $CD4^+$ and B cell subset depletion did not markedly influence the kinetics of prolonged chronic liver disease (8).

The remarkable increase in the frequencies of intrahepatic monocytes/macrophages was observed in the inflamed transgenic mice. In the previous observation of acute liver injury, intrahepatic monocytes/macrophages were recruited from the circulation and activated by IFNγ secreted from the CTLs (7). Although similar mechanisms were speculated, further studies are required to determine the functional properties of intrahepatic monocytes/macrophages in the development of chronic hepatitis and HCC.

References

1. Di Bisceglie A.M.: Hepatitis C and hepatocellular carcinoma. Hepatology 26: 34S-38S, 1997.
2. Ikeda K., Saitoh S., Suzuki Y., et al.: Disease progression and hepatocellular carcinogenesis in patients with chronic viral hepatitis: a prospective observation of 2215 patients. J. Hepatol. 28: 930-938, 1998.
3. Chisari F.V., Klopchin K., Moriyama T., et al.: Molecular pathogenesis of hepatocellular carcinoma in hepatitis B virus transgenic mice. Cell 59: 1145-1156, 1989.
4. Nakamoto Y., Guidotti L.G., Kuhlen C.V., Fowler. P., Chisari, F. V.: Immune pathogenesis of hepatocellular carcinoma. J. Exp. Med. 188: 341-350, 1998.
5. Chisari F.V., Filippi P., McLachlan A., et al.: Expression of hepatitis B virus large envelope polypeptide inhibits hepatitis B surface antigen secretion in transgenic mice. J. Virol. 60: 880-887, 1986.
6. Moriyama T., Guilhot S., Klopchin K., et al.: Immunobiology and pathogenesis of hepatocellular injury in hepatitis B virus transgenic mice. Science 248: 361-364, 1990.
7. Ando K., Moriyama T., Guidotti L.G., et al.: Mechanisms of class I restricted immunopathology. A transgenic mouse model of fulminant hepatitis. J. Exp. Med. 178: 1541-1554. 1993.
8. Nakamoto Y., Suda T., Momoi T., Kaneko S.: Different procarcinogenic potentials of lymphocyte subsets in a transgenic mouse model of chronic hepatitis B. Cancer Res. 64: 3326-3333, 2004.

Received: July, 20, 2005

Yasunari Nakamoto, M.D.,Ph.D.
Department of Gastroenterology,
Graduate School of Medicine, Kanazawa University,
13-1 Takara-machi, Kanazawa 920-8641, Japan
Tel: 81-76-265-2243, Fax: 81-76-234-4250
E-mail: ynakamot@medf.m.kanazawa-u.ac.ja

Cytotoxic T Cell Responses to Human Telomerase Reverse Transcriptase in Patients With Hepatocellular Carcinoma

Eishiro Mizukoshi,[1] Yasunari Nakamoto,[1] Yohei Marukawa,[1] Kuniaki Arai,[1] Tatsuya Yamashita,[1] Hirokazu Tsuji,[1] Kiyotaka Kuzushima,[2] Masafumi Takiguchi,[3] and Shuichi Kaneko[1]

Human telomerase reverse transcriptase, hTERT, has been identified as the catalytic enzyme required for telomere elongation. hTERT is expressed in most tumor cells but seldom expressed in most human adult cells. It has been reported that 80% to 90% of hepatocellular carcinomas (HCCs) express hTERT, making the enzyme a potential target in immunotherapy for HCC. In the current study, we identified hTERT-derived, HLA-A*2402–restricted cytotoxic T cell (CTL) epitopes and analyzed hTERT-specific CTL responses in patients with HCC. Peptides containing the epitopes showed high affinity to bind HLA-A*2402 in a major histocompatibility complex binding assay and were able to induce hTERT-specific CTLs in both hTERT cDNA-immunized HLA-A*2402/K^b transgenic mice and patients with HCC. The CTLs were able to kill hepatoma cell lines depending on hTERT expression levels in an HLA-A*2402–restricted manner and induced irrespective of hepatitis viral infection. The number of single hTERT epitope-specific T cells detected by ELISPOT assay was 10 to 100 specific cells per 3×10^5 PBMCs, and positive T cell responses were observed in 6.9% to 12.5% of HCC patients. hTERT-specific T cell responses were observed even in the patients with early stages of HCC. The frequency of hTERT/tetramer$^+$CD8$^+$ T cells in the tumor tissue of patients with HCC was quite high, and they were functional. In conclusion, these results suggest that hTERT is an attractive target for T-cell–based immunotherapy for HCC, and the identified hTERT epitopes may be valuable both for immunotherapy and for analyzing host immune responses to HCC. (HEPATOLOGY 2006;43:1284-1294.)

Hepatocellular carcinoma (HCC) is the most frequent primary malignancy of the liver and has gained much clinical interest because of its increasing incidence.[1-3] Although current advances in therapeutic modalities have improved the prognosis of HCC patients,[4-6] the survival rate is still not satisfactory. One of the reasons for the poor prognosis is the high rate of recurrence after treatment. To protect against recurrence, tumor antigen-specific immunotherapy is an attractive strategy. Although many tumor-specific antigens have been identified in various cancers, the number of HCC-specific antigens known is still limited.

Human telomerase reverse transcriptase, hTERT, has been identified as the catalytic enzyme required for telomere elongation.[7-10] Recently, several results regarding hTERT-specific cytotoxic T cell (CTL) responses were reported for humans and mice.[11-20] These reports revealed that hTERT-specific CTLs induced by stimulation with peptides or DNA-based immunization kill cancer cell lines that have high levels of hTERT, suggesting that hTERT-reactive T cell clones are not deleted from the human T cell repertoire and that hTERT may be a useful tumor-specific antigen as a target for T-cell–based immunotherapy for cancers. However, the existence of hTERT-specific CTLs and the relationship between immunological

Abbreviations: HCC, hepatocellular carcinoma; hTERT, human telomerase reverse transcriptase; CTL, cytotoxic T cell; HIV, human immunodeficiency virus; PBMC, peripheral blood mononuclear cell; AFP, alpha-fetoprotein; CMV, cytomegalovirus; FCS, fetal calf serum; TIL, tumor infiltrating lymphocyte; PCR, polymerase chain reaction; TRAP, telomerase repeat amplification protocol; IFN-γ, interferon gamma.

From the [1]Department of Gastroenterology, Graduate School of Medicine, Kanazawa University, Kanazawa, Ishikawa, Japan; the [2]Division of Immunology, Aichi Cancer Center Research Institute, Aichi Cancer Center Hospital, Nagoya, Aichi, Japan; and the [3]Division of Viral Immunology, Center for AIDS Research, Kumamoto University, Honjo, Kumamoto, Japan.

Received August 8, 2005; accepted March 20, 2006.

Address reprint requests to: Shuichi Kaneko, M.D., Department of Gastroenterology, Graduate School of Medicine, Kanazawa University, Kanazawa, Ishikawa 920-8641, Japan. E-mail: skaneko@medf.m.kanazawa-u.ac.jp; fax: 81-76-234-4250.

Published online in Wiley InterScience (www.interscience.wiley.com).

DOI 10.1002/hep.21203

Potential conflict of interest: Nothing to report.

responses and clinical factors have not been well characterized in patients with HCC.

In the current study, we first attempted to identify HLA-A*2402–restricted T cell epitopes derived from hTERT and then analyzed hTERT-specific immunological responses in HCC patients.

Patients and Methods

Patient Population. The study examined 72 HLA-A24–positive patients with HCC who were admitted to Kanazawa University Hospital between January 2002 and December 2004, consisting of 48 men and 24 women ranging from 46 to 81 years of age with a mean age of 67 ± 9 years. HCCs were detected by imaging modalities such as dynamic computed tomography (CT) scan, magnetic resonance imaging, and abdominal arteriography. The diagnosis of HCC was histologically confirmed by taking ultrasound-guided needle biopsy specimens in 29 cases, surgical resection in four cases, and autopsy in four cases. For the remaining 35 patients, the diagnosis was based on typical hypervascular tumor staining on angiography in addition to typical findings, which showed hyperattenuated areas in the early phase and hypoattenuation in the late phase on dynamic CT.[21] All subjects were negative for antibodies to human immunodeficiency virus (HIV) and gave written informed consent to participate in this study in accordance with the Helsinki declaration. Eleven healthy blood donors with HLA-A24, who did not have a history of cancer and were negative for hepatitis B surface antigen and anti-HCV antibody, served as controls.

Laboratory and Virologic Testing. Blood samples were tested for hepatitis B surface antigen and HCV antibody by commercial immunoassays (Fuji Rebio, Tokyo, Japan). HLA-based typing of peripheral blood mononuclear cells (PBMCs) from patients and normal donors was performed using complement-dependent microcytotoxicity with HLA typing trays purchased from One Lambda.

The serum alpha-fetoprotein (AFP) level was measured by enzyme immunoassay (AxSYM AFP, Abbott Japan, Tokyo, Japan), and the pathological grading of tumor cell differentiation was assessed according to the general rules for the clinical and pathological study of primary liver cancer.[22] The severity of liver disease (stage of fibrosis) was evaluated according to the criteria of Desmet et al.,[23] using biopsy specimens of liver tissue, where F4 was defined as cirrhosis.

Synthetic Peptides. To identify potential HLA-A24–binding peptides within hTERT, the sequence was reviewed using a computer-based program, which was employed by accessing the World Wide Web site BioInformatics and Molecular Analysis Section for HLA peptide binding predictions (available from http://bimas.cit.nih.gov). The HLA-A24–restricted epitopes derived from HIV envelope protein,[24] cytomegalovirus (CMV) pp65,[25] and HCV NS3 were used as control peptides to test for T cell responses, and the HLA-A2–restricted epitope derived from AFP[26] was used as a control peptide for HLA-A24 stabilization assay as previously described. Peptides were synthesized at Mimotope (Melbourne, Australia) and Sumitomo Pharmaceuticals (Osaka, Japan). They were identified using mass spectrometry, and their purities were determined to be greater than 80% by analytical high-pressure liquid chromatography.

Cell Lines. Three human hepatoma cell lines, HepG2, HuH6, and HuH7, were cultured in Dulbecco's minimum essential medium (Gibco, Grand Island, NY) with 10% fetal calf serum (FCS) (Gibco).

T2-A24 cells, which were T2 cells transfected with HLA-A*2402,[25] were cultured in RPMI 1640 medium containing 10% FCS and 800 μg/mL G418 (GibcoBRL, Grand Island, NY). The HLA-A*2402 gene-transfected C1R cell line (C1R-A24)[27] was cultured in RPMI 1640 medium containing 10% FCS and 500 μg/ml of hygromycin B(Sigma, St Louis, MO), and K562 was cultured in RPMI 1640 medium containing 10% FCS. All media contained 100 U/mL penicillin and 100 μg/mL streptomycin (GibcoBRL, Grand Island, NY).

Plasmid Construction. The plasmid which contains hTERT cDNA was subcloned as previously described.[28] In brief, the EcoRI-SalI fragment containing the hTERT cDNA was subcloned from pCI-Neo-hTERT, which was provided by Dr. Seishi Murakami (Cancer Research Institute, Kanazawa University). The fragment was subcloned into the EcoRI-SalI sites of the plasmid pNKZ-FLAG (pNKZ-FLAG-hTERT).

Injection of hTERT cDNA Into HLA-A*2402/K^b Transgenic Mice. Transgenic mice expressing the α1 and α2 domains from the HLA-A*2402 molecule and the α3 domain from the murine H-2K^b molecule,[29] kindly provided by Sumitomo Pharmaceuticals (Osaka, Japan), were bred in a specific-pathogen–free environment at the animal facility in Kanazawa University. For immunization with the hTERT cDNA, mice were injected with 50 μL cardiotoxin (Latoxan, Rosans, France) (10 μmol/L) per leg into the tibialis anterior muscles on both sides. Five days after injection of the cardiotoxin, the vector pNKZ-FLAG-hTERT containing the hTERT cDNA was injected into the same part of the muscle. Mice immunized with the plasmid pNKZ-FLAG were also used as negative controls. Splenocytes harvested on day 7 after the

Table 1. Characteristics of the Patients Studied

Clinical Diagnosis	No. of Patients	Sex M/F	Age (yr) Mean ± SD	ALT (IU/L) Mean ± SD	AFP (ng/mL) Mean ± SD	Etiology (B/C/Others)	Child-Pugh (A/B/C)	Diff. degree* (Wel/Mod/ Por/ND)	Tumor size** (Large/ Small)	Tumor multiplicity (Multiple/ Solitary)	Vascular invasion (+/−)	TNM Stage (I/II/IIIA/ IIIB/IIIC/IV)
HCC patients	72	48/24	67 ± 9	66 ± 36	1722 ± 7029	9/59/4	43/25/4	15/21/1/35	44/28	39/33	15/57	30/26/9/1/2/4
Normal donors	11	8/3	35 ± 2	ND	ND	ND	ND	ND	ND	ND	ND	ND

*Histological degree of HCC; wel: well differentiated, mod: moderately differentiated, por: poorly differentiated. ND: not determined.
**Tumor size was divided into either "small" (≤2 cm) or "large" (> 2 cm).

injection of cDNA were tested directly *ex vivo* for IFN-γ production using an ELISPOT assay.

Preparation of PBMCs and Tumor-Infiltrating Lymphocytes. PBMCs were isolated as previously described.[30,31] Fresh PBMCs were used for the CTL assay, and the remaining PBMCs were resuspended in RPMI 1640 medium containing 80% FCS and 10% dimethyl sulfoxide (Sigma, St. Louis, MO) and cryopreserved until used. Tumor-infiltrating lymphocytes (TILs) were isolated by mechanical homogenization of tumors, which were resected by surgical treatment and cryopreserved as described until used.

Major Histocompatibility Complex Binding Assay. Peptide binding assays were performed as previously described.[31,32] The data were expressed as % mean fluorescence intensity (MFI) increase, which was calculated as follows: Percent MFI increase = (MFI with the given peptide − MFI without peptide)/(MFI without peptide) × 100.

ELISPOT Assay. ELISPOT assays were performed as previously described[31] with the following modifications. Three hundred thousand unfractionated PBMCs or 100,000 TILs with 10,000 T2-A24 cells were added in duplicate cultures of RPMI 1640 medium containing 5% FCS together with the peptides at 10 μg/mL. For the mouse assay, 2×10^5 spleen cells were used for each well. The number of specific spots was determined by subtracting the number of spots in the absence of antigen from that in the presence of antigen. Responses were considered positive for the human ELISPOT assay if more than 10 specific spots were detected and if the number of spots in the presence of antigen was at least twofold greater than that in the absence of antigen.

Cytotoxicity Assay. hTERT-derived peptide-specific T cells were expanded from PBMCs in 96-well round-bottomed plates (NUNC, Naperville, IL) as previously described.[30] Briefly, 400,000 cells per well were stimulated with 10 μg/mL synthetic peptide, 10 ng/mL rIL-7, and 100 pg/mL rIL-12 (Sigma) in RPMI 1640 medium supplemented with 10% heat-inactivated human AB serum, 100 U/mL penicillin, and 100 μg/mL streptomycin. The cultures were re-stimulated with 10 μg/mL peptide, 20 U/mL of rIL-2 (Sigma) and 1×10^5 mytomicin C-treated autologous PBMCs on days 7 and 14. On days 3, 10, and 17, 100 μL RPMI with 10% human AB serum and 10 U/mL rIL-2 (final concentration) were added to each well. Cytotoxicity assays were performed as previously described.[31]

Tetramer Staining and Flow Cytometry. Peptide $hTERT_{461}$-specific tetramer was purchased from Medical Biological Laboratories Co., Ltd (Nagoya, Japan). Tetramer staining was performed as previously described.[33] In brief, PBMCs and TILs were stained with CD4-FITC, CD14-FITC, CD19-FITC, CD8-PerCP (BD PharMingen, San Diego, CA), and tetramer-PE (10 μL) for 30 minutes at room temperature. Cells were washed, fixed with 0.5% paraformaldehyde/phosphate-buffered saline, and analyzed on a FACSCalibur flow cytometer. Data analysis was undertaken with CELLQuest software (Becton Dickinson, San Jose, CA).

Telomerase Assay. Telomerase activity was measured by two methods according to the manufacturer's directions. First, a polymerase chain reaction (PCR)-based telomerase repeat amplification protocol (TRAP) assay was carried out with a TRAPEZE ELISA telomerase detection kit (Intergen Co. Ltd., Auckland, New Zealand). The products of the PCR were fractionated by electrophoresis on a 10% polyacrylamide gel and then visualized by staining with SYBR-Green I (Molecular Probes, Eugene OR). Second, a TRAP enzyme-linked immunosorbent assay (ELISA) was used to quantitatively measure telomerase activity with a TRAPEZE ELISA telomerase detection kit (Intergen Co. Ltd.). Cell extracts were prepared from HepG2, HuH6, and HuH7 cells and used at 0.01 μg per assay. Telomerase activity was also measured in the tumor of 10 patients with HCC who received surgical treatment. Cell extracts were prepared from resected tumors and used at 0.1 μg per assay.

Statistical Analysis. Fisher's exact test (2-sided *P*-value) and the unpaired Student's *t* test were used to analyze the effect of variables on immune responses in HCC patients.

Results

Patient Profiles. The clinical profiles of the patients are shown in Table 1. The tumors of 37 patients were

Table 2. Peptides

Peptide	Source	Start Position	Amino Acid Sequence	HLA Restriction	Score*
$hTERT_{1088}$	hTERT	1088	TYVPLLGSL	HLA-A24	432
$hTERT_{845}$	hTERT	845	CYGDMENKL	HLA-A24	317
$hTERT_{167}$	hTERT	167	AYQVCGPPL	HLA-A24	300
$hTERT_{461}$	hTERT	461	VYGFVRACL	HLA-A24	280
$hTERT_{324}$	hTERT	324	VYAETKHFL	HLA-A24	240
$hTERT_{1009}$	hTERT	1009	AYRFHACVL	HLA-A24	200
$hTERT_{385}$	hTERT	385	RYWQMRPLF	HLA-A24	200
$hTERT_{637}$	hTERT	637	DYVVGARTF	HLA-A24	150
$hTERT_{622}$	hTERT	622	RFIPKPDGL	HLA-A24	72
$hTERT_{869}$	hTERT	869	DFLLVTPHL	HLA-A24	42
HIV env_{584}	HIV envelope	584	RYLRDQQLL	HLA-A24	720
CMV $pp65_{328}$	CMV pp65	328	QYDPVAALF	HLA-A24	168
HCV $NS3_{1031}$	HCV NS3	1031	AYSQQTRGL	HLA-A24	200
AFP_{137}	AFP	137	PLFQVPEPV	HLA-A2	3

*Estimated half-time of dissociation from the HLA-A24 or -A2 allele (min).

histologically classified as 15 well, 21 moderately, and 1 poorly differentiated HCC. Other patients were diagnosed with HCC based on typical CT findings and an elevation of AFP. The tumors were categorized as "large" (>2 cm) in 44 cases and "small" (≤2 cm) in 28 cases, and as "multiple" (≥2 nodules) in 39 cases and "solitary" (single nodule) in 33 cases. Vascular invasion of the HCC was observed in 15 cases. According to the TNM staging of the Union Internationale Contre Le Cancer (UICC) classification system (6th version),[34] 30, 26, 9, 1, 2, and 4 patients were classified as having stages I, II, IIIA, IIIB, IIIC, and IV disease, respectively.

Selection of Potential HLA-A24–Binding Peptides Within hTERT. To identify potential HLA-A24–binding peptides, the amino acid sequences of hTERT were analyzed using a computer program designed to predict HLA-binding peptides based on the estimation of the half-time dissociation of the HLA–peptide complex. Ten peptides were selected according to the half-time dissociation scores (Table 2). Two of the 10 peptides have been reported to contain HLA-A*2402–restricted epitopes (peptides $hTERT_{461}$ and $hTRERT_{324}$).[35] Next, MHC stabilization assays were performed to test the HLA-A*2402–binding capacity of these peptides using T2-A24 cells. Most peptides increased HLA-A24 expression, indicating that they bound and stabilized the HLA complex on the cell surface (Fig. 1). Peptide CMV$pp65_{328}$, which is identified as a strong binder of the HLA-A*2402 molecule,[25] also increased HLA-A24 expression. Percent MFI increase of the tested peptides except for peptides $hTERT_{1009}$, $hTERT_{385}$, and $hTERT_{622}$ was greater than that of peptide AFP_{137}, which is HLA-A2 restricted.[26]

Immunogenicity of hTERT Peptides in HLA-A*2402/K^b Transgenic Mice. To determine whether these HLA-A24–binding peptides include HLA-A*2402–restricted T cell epitopes, HLA-A*2402/K^b transgenic mice were immunized with hTERT cDNA, and the spleen cell responses were evaluated by interferon gamma (IFN-γ) ELISPOT. Six of 10 hTERT-derived peptides were recognized by the spleen cells of at least one of the primed mice (Fig. 2). Peptides $hTERT_{1009}$, $hTERT_{385}$, $hTERT_{622}$, and $hTERT_{869}$ were not recognized by any mice. These results show that peptides $hTERT_{1088}$, $hTERT_{845}$, $hTERT_{167}$, $hTERT_{461}$, $hTERT_{324}$, and $hTERT_{637}$ may be immunogenic and contain the epitopes restricted by HLA-A*2402.

T Cell Responses to hTERT-Derived Peptides Assessed by IFN-γ ELISPOT Analysis in HCC Patients. To determine whether these HLA-A24–binding peptides could be recognized by the T cells of patients with HCC, PBMC responses were evaluated by IFN-γ ELISPOT. Six of 10 hTERT-derived peptides were recognized by PBMCs of at least one patient, and 29 of 72 patients (40.3%) responded to at least one of the analyzed hTERT-derived peptides. An overview of all responses is shown in Fig. 3A. Single hTERT epitope-specific IFN-γ–producing cells were detected in 6 (8.3%), 6 (8.3%), 9 (12.5%), 5 (6.9%), 9 (12.5%), and 9 (12.5%) of 72 patients in response to the stimulation with peptides $hTERT_{1088}$, $hTERT_{845}$, $hTERT_{167}$, $hTERT_{461}$, $hTERT_{324}$, and $hTERT_{637}$, respectively. Peptides $hTERT_{1009}$, $hTERT_{385}$, $hTERT_{622}$, and $hTERT_{869}$ were not recognized by any patient.

The peptides recognized by PBMCs of the patients with HCC were comparable to those recognized by spleen cells of hTERT cDNA-immunized HLA-A*2402/K^b transgenic mice. These peptides also displayed a relatively high affinity for the HLA-A*2402 molecule compared with the negative control peptide (Fig. 1). The strength of the hTERT-specific T cell responses assessed by the frequencies of IFN-γ–producing cells in the PBMC population is between 10 and 100 specific cells per 3×10^5 PBMCs. Peptide CMV$pp65_{328}$, which includes an

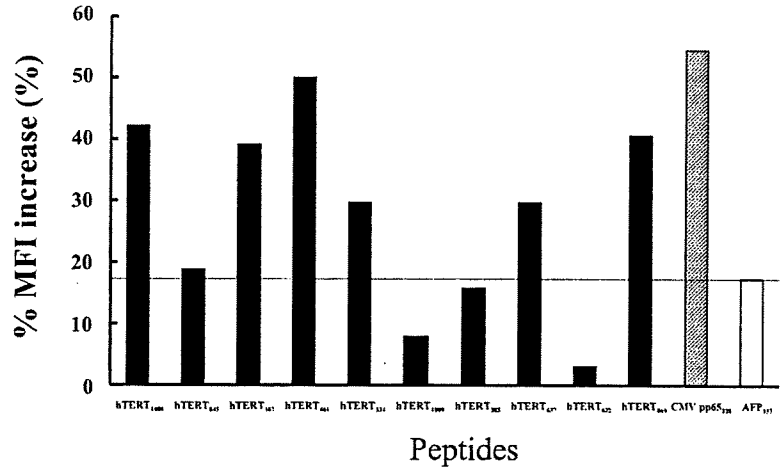

Fig. 1. MHC binding affinity. TAP-deficient T2-A24 cells were cultured for 16 hours at 26°C to enhance the expression of peptide-receptive cell surface molecules. They were incubated with individual peptides at 10 μg/mL at 37°C for 2 hours, washed, and stained with anti-HLA-A24 monoclonal antibody, anti-mouse immunoglobulin-conjugated FITC, and 1 μg propidium iodide per milliliter. The data are expressed as the percent mean fluorescence intensity (MFI) increase for live, propidium iodide-negative cells. Peptide CMVpp65$_{328}$, a previously identified CMV pp65-derived peptide known to be a strong binder to HLA-A24, was used as a positive control. Peptide AFP$_{137}$, a previously identified AFP-derived peptide known to be HLA-A2 restricted, was used as a negative control. The experiment was performed three times, and a representative result is shown. MHC, major histocompatibility complex; HLA, human leukocyte antigen; FITC, fluorescein isothiocyanate; CMV, cytomegalovirus.

epitope derived from the CMV pp65 protein, and HCVNS3$_{1031}$, which includes an epitope derived from the HCV NS3 protein, were also recognized by PBMCs of 31 of 72 (40%) and 12 of 51 (24%) patients with HCC, respectively. Conversely, no patients showed positive T cell responses against peptide HIVenv$_{584}$ derived from the HIV envelope protein, suggesting that these T cell responses were antigen-specific.

In contrast to the results for HCC patients, the ELISPOT assays for the healthy donors did not show more than 10 specific spots for all hTERT-derived peptides (Fig. 3B). The numbers of specific spots (mean ± SD) in the healthy donors were 1.4 ± 1.7, 0.6 ± 0.8, 0.8 ± 1.1, 0.7 ± 1.2, 0.5 ± 0.7, 0.6 ± 1.2, 2.0 ± 2.6, 1.7 ± 2.6, 1.6 ± 3.4, and 1.9 ± 2.9 for hTERT$_{1088}$, hTERT$_{845}$, hTERT$_{167}$, hTERT$_{461}$, hTERT$_{324}$,

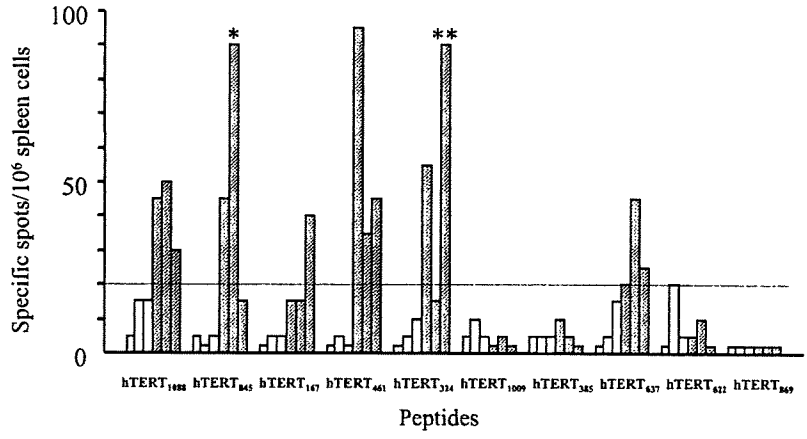

Fig. 2. Direct *ex vivo* analysis (IFN-γ ELISPOT assay) of spleen cell responses to hTERT-derived peptides in hTERT cDNA (hatched bars) or β-gal cDNA (open bars)-immunized HLA-A*2402/K^b transgenic mice. The immunization was performed in three mice for each cDNA. A positive T cell response was defined as more than 20 specific spots/1 × 10^6 spleen cells, which was the maximum response in β-gal cDNA-immunized mice. The peptide sequences are described in Table 2. * denotes 450 specific spots, ** denotes 130 specific spots. IFN-γ, interferon gamma; hTERT, human telomerase reverse transcriptase.

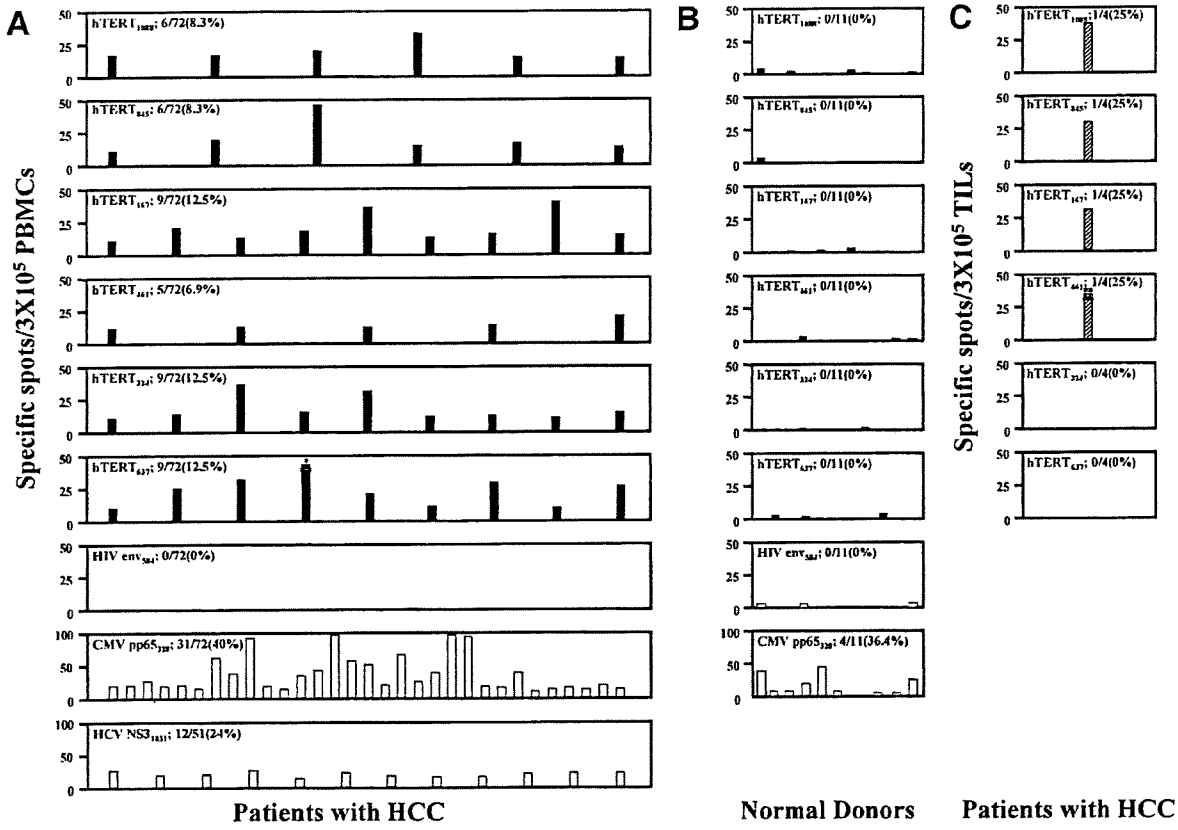

Fig. 3. Direct *ex vivo* analysis (IFN-γ ELISPOT assay) of peripheral blood T cell responses to hTERT-derived peptides (peptides $hTERT_{1088}$, $hTERT_{845}$, $hTERT_{167}$, $hTERT_{461}$, $hTERT_{324}$, and $hTERT_{637}$; solid bars) or control peptides (Peptides $HIVenv_{584}$, $CMVpp65_{328}$ and $HCVNS3_{1031}$; open bars) in HCC patients (A) and normal donors (B). Direct *ex vivo* analysis of tumor-infiltrating lymphocyte responses to hTERT-derived peptides (hatched bars) in HCC patients (C). Only significant IFN-γ responses are included in A and C. Responses were considered positive if more than 10 specific spots were detected and if the number of spots in the presence of antigen was at least twofold greater than that in the absence of antigen. The peptide sequences are described in Table 2. The data for peptides $hTERT_{1009}$, $hTERT_{385}$, $hTERT_{622}$, and $hTERT_{869}$ are excluded because there was no positive T cell response. * denotes 100 specific spots. ** denotes 243 specific spots. IFN-γ, interferon gamma; hTERT, human telomerase reverse transcriptase; HCC, hepatocellular carcinoma.

$hTERT_{1009}$, $hTERT_{385}$, $hTERT_{637}$, $hTERT_{622}$, and $hTERT_{869}$ peptides, respectively. The proportion of normal donors who showed positive T cell responses to CMV protein-derived peptides and the frequencies of the specific T cells were virtually the same as those of the HCC patients (Fig. 3B).

In ELISPOT assay using TILs, IFN-γ–producing T cells responding to peptides $hTERT_{1088}$, $hTERT_{845}$, $hTERT_{167}$, and $hTERT_{461}$ were detected as shown in Fig 3C, suggesting that hTERT-specific TILs were functional.

Cytotoxic Activity Against hTERT-Derived Peptides in HCC Patients. All hTERT-derived peptides were tested for their potential to induce HLA-A24–restricted CTLs from PBMCs of HCC patients with HLA-A24. Each peptide was tested on at least 10 patients. After three rounds of stimulation with the synthetic peptides, responder cells that had been stimulated with peptides $hTERT_{1088}$, $hTERT_{845}$, $hTERT_{167}$, $hTERT_{461}$, $hTERT_{324}$, and $hTERT_{637}$ lysed the peptide-pulsed C1R-A*2402 cells as shown in Fig. 4. Conversely, other peptides failed to induce CTLs specific for the corresponding peptides.

Cytotoxic Activity of hTERT Peptide-Specific CTLs Against Hepatoma Cell Lines. To examine whether hTERT peptide-specific CTLs induced from PBMCs of HCC patients lyse hepatoma cell lines that express hTERT, we first checked the telomerase activity in three hepatoma cells. TRAP assays showed that the three hepatoma cells expressed hTERT; however, the expression in HuH6 cells was lower than that in HepG2 or HuH7 cells (Fig. 5A). The results were confirmed in the TRAP ELISA, which is a quantitative measurement of telomerase activity. The expression levels of hTERT in HepG2 and HuH7 cells were more than twofold higher than the level in HuH6 cells (Fig. 5B).

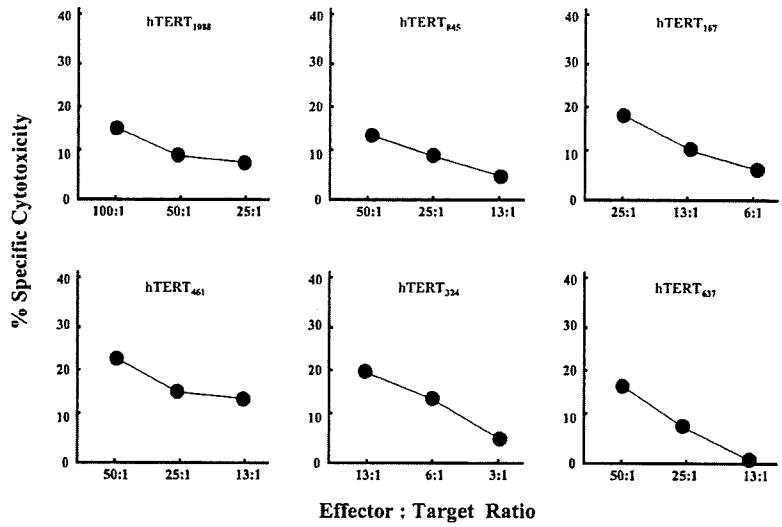

Fig. 4. Cytotoxicity of hTERT-specific T-cell lines derived with peptide in patients with HCC. The cytotoxicity of the T-cell lines was determined by a standard 6-hour cytotoxicity assay at various effector to target (E/T) ratios against C1R-A*2402 cells pulsed with one of the hTERT-derived peptides listed in Table 2. The data are indicated as the percent specific cytotoxicity, which is calculated as follows: (cytotoxicity in the presence of specific peptide) − (cytotoxicity in the absence of peptide). hTERT, human telomerase reverse transcriptase; HCC, hepatocellular carcinoma.

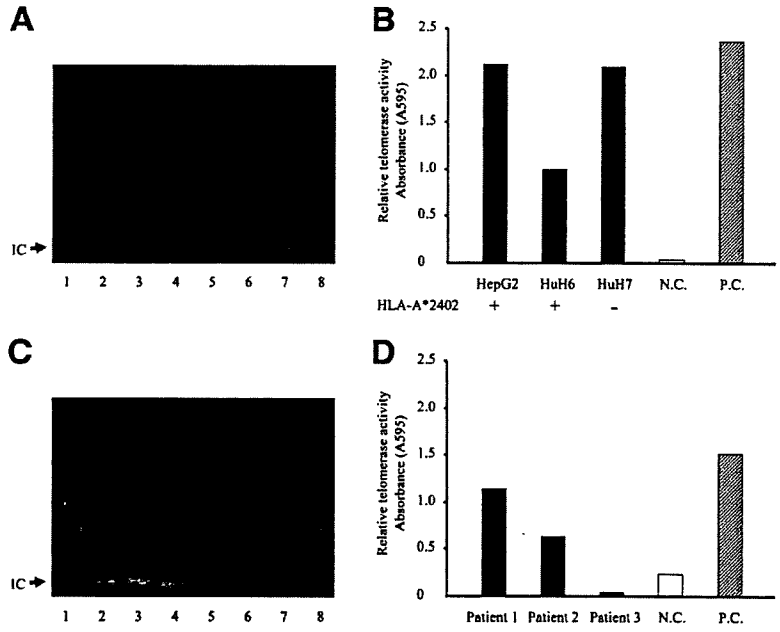

Fig. 5. Telomerase activity in hepatoma cell lines (A, B) and tumors resected by surgical treatment (C, D). A TRAP assay was carried out with 0.01 μg and 0.1 μg cell extract from hepatoma cell lines and tumors, respectively. The products of the PCR were fractionated by electrophoresis on a 10% polyacrylamide gel and then visualized by staining with SYBR-Green I. The TRAP internal control (IC) is shown for each extract. A: Lane 1; HepG2, Lane 2; HepG2 with heat, Lane 3; HuH 6, Lane 4; HuH 6 with heat, Lane 5; HuH 7, Lane 6; HuH 7 with heat, Lane 7; negative control, Lane 8; positive control. B: Lanes 1, 3, and 5, HCCs from three different patients; Lanes 2, 4, and 6, HCCs from three different patients with heat; Lane 7, negative control; Lane 8, positive control. Relative telomerase activity was measured with a TRAPEZE ELISA telomerase detection kit (TRAP ELISA) in hepatoma cell lines (C) and tumors resected by surgical treatment (D). Molecular typing of the HLA-A allele for hepatoma cell lines was performed with genomic DNA using standard site-specific oligonucleotide PCR. NC, negative control; PC, positive control; TRAP, telomerase repeat amplification protocol; PCR, polymerase chain reaction; HCC, hepatocellular carcinoma.

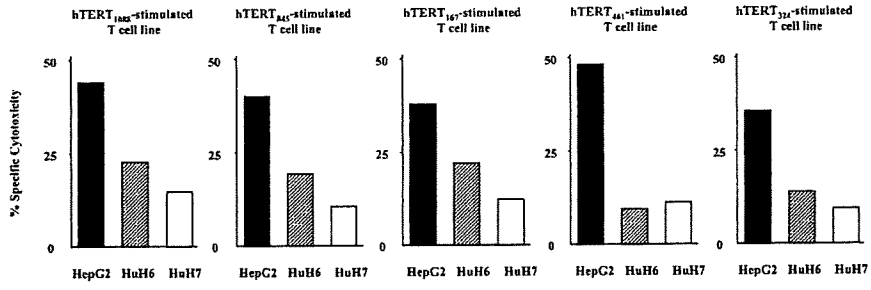

Fig. 6. Cytotoxicity of hTERT-specific T-cell lines derived with peptide against hepatoma cell lines. HepG2 (solid bar) highly expresses hTERT and has HLA-A*2402. HuH 6 (hatched bar) shows low expression of hTERT and has HLA-A*2402. HuH 7 (open bar) shows hTERT expression of the same level as HepG2 but does not have HLA-A*2402. The cytotoxicity was determined by a standard 6-hour cytotoxic assay (E/T ratio of 50:1). hTERT, human telomerase reverse transcriptase.

We next examined the cytotoxicity of hTERT peptide–specific CTLs against these hepatoma cell lines. As shown in Fig. 6, peptides $hTERT_{1088}$, $hTERT_{845}$, $hTERT_{167}$, $hTERT_{461}$, and $hTERT_{324}$-specific CTLs showed cytotoxicity against HepG2 cells, which highly express hTERT and has the HLA-A*2402 molecule. In contrast, the CTLs did not show cytotoxicity against HuH7 cells, which express hTERT at the same level as HepG2 cells but do not have HLA-A*2402. In addition, the cytotoxicity of hTERT-specific CTLs induced with peptides $hTERT_{1088}$, $hTERT_{845}$, $hTERT_{167}$, and $hTERT_{324}$ against HuH6 cells, which express HLA-A*2402 and a low level of hTERT, was weak compared with the cytotoxicity against HepG2 cells. The difference was even more marked in the cytotoxicity of CTLs induced with peptide $hTERT_{461}$, and the CTLs were not cytotoxic to HuH6 cells.

Telomerase activity was also detected in the tumor of 3 of 10 patients with HCC (Fig. 5C and D). All of the three patients showed hTERT-specific T cell responses in ELISPOT assay.

Detection of $hTERT_{461}$ Tetramer$^+$ and CD8$^+$ T Lymphocytes in PBMCs and TILs. To analyze the character of hTERT specific T cells in patients with HCC more precisely, we examined the frequencies of $hTERT_{461}$ tetramer$^+$ cells in PBMCs and TILs, and compared them with the results of ELISPOT assay. PBMCs and TILs were stained with CD4-FITC, CD14-FITC, CD19-FITC, CD8-PerCP, and tetramer-PE as described in Patients and Methods. At least 1×10^5 cells in the $CD8^+CD4^-CD14^-CD19^-$ gate were then analyzed for tetramer staining as shown in Fig. 7A.

As indicated in Fig. 7B, the frequencies of $CD8^+$ $CD4\text{-}CD14^-CD19^-hTERT_{461}$ tetramer$^+$ cells in peripheral blood were 0.03% to 0.71% of $CD8^+$ T cells (patients 1-15). The frequencies in the patients with positive responses for ELISPOT assay were 0.06% to 0.71%. Interestingly, 7 of 10 patients without positive responses for ELISPOT assay showed 0.07% to 0.26% $CD8^+$ $CD4^-CD14^-CD19^-hTERT_{461}$tetramer$^+$ cells. These results suggest that dysfunctional hTERT-specific T cells exist in patients with HCC. Conversely, the frequency of $CD8^+CD4^-CD14^-CD19^-hTERT_{461}$ tetramer$^+$ cells in TILs was quite high (2.73%), and they were functional (patient 16).

hTERT-Specific T Cell Responses and Clinical Features of HCC Patients. To evaluate the status of hTERT-specific T cell responses in patients with HCC,

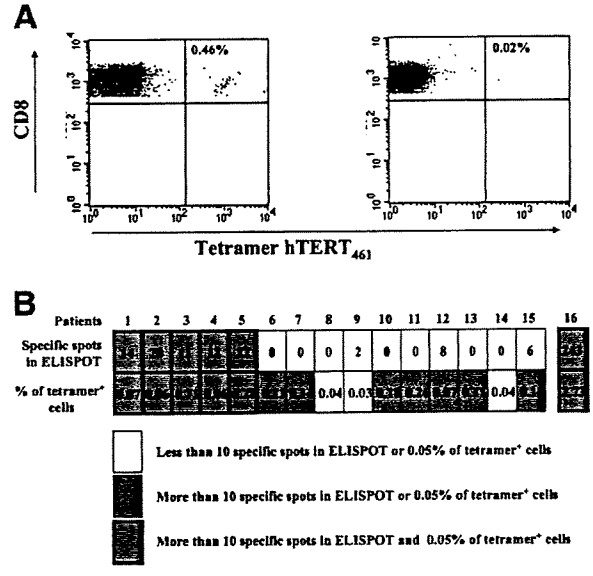

Fig. 7. Detection of hTERT-specific, HLA-A*2402-tetramer$^+$, $CD8^+CD4^-CD14^-$ $CD19^-$ T lymphocytes in the peripheral blood and tumor. PBMCs isolated from representative patients with HCC (A) were stained with tetrameric complexes and antibodies and analyzed on a FACSCalibur™ flow cytometer. Analysis of the association between the frequency of tetramer$^+$ cells and IFN-γ-producing cells detected in ELISPOT assay (B). Tetramer staining and ELISPOT assay were performed in 16 patients using PBMCs (patients 1-15) and TILs (patient 16). hTERT, human telomerase reverse transcriptase; PBMC, peripheral blood mononuclear cell; HCC, hepatocellular carcinoma; IFN-γ, interferon gamma; TIL, tumor-infiltrating lymphocyte.

Table 3. Univariate Analysis of the Effect of Variables on the T Cell Response Against hTERT

	Patients With Positive T Cell Response	Patients Without Positive T Cell Response	P
No. of patients	29	43	
Age (years)*	67.7 ± 9.7	66.7 ± 8.1	NS
Sex (M/F)	21/8	27/16	NS
AFP level (≦20/> 20)	13/16	14/29	NS
Diff. degree of HCC (well/ moderate or poor/ND[c])	9/6/14	6/16/21	NS
Tumor multiplicity (multiple/ solitary)	17/12	22/21	NS
Vascular invasion (+/−)	7/22	8/35	NS
TNM factor			
(T1/T2-4)	11/18	19/24	NS
(N0/N1)	28/1	43/0	NS
(M0/M1)	29/0	39/4	NS
TNM stage (I/II-IV)	11/18	19/24	NS
Histology of non-tumor liver (LC/Chronic hepatitis)	25/4	39/4	NS
Liver function (Child A/B/C)	13/14/2	30/11/2	NS
Etiology (HCV/HBV/Others)	22/3/4	37/6/0	NS

Abbreviations: NS; there was no statistical significance; ND, not determined.
*Data are expressed as mean ± SD.

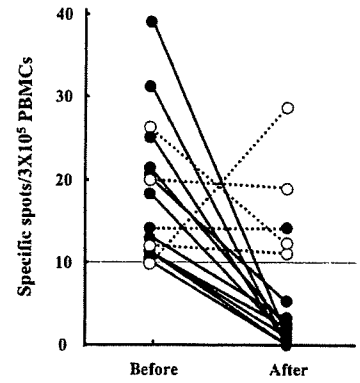

Fig. 8. Kinetics of hTERT-specific T cell responses before and after curative treatments. PBMCs were obtained before and 6 months after treatments and analyzed. Open circles show the patients without tumor recurrence within 1 year after treatment. Closed circles show the patients with tumor recurrence within 1 year after treatment. Solid and dotted lines show the patients without and with more than 10 specific spots for hTERT-derived peptides in ELISPOT assay after treatment, respectively. hTERT, human telomerase reverse transcriptase; PBMC, peripheral blood mononuclear cell.

we analyzed the relationship between the frequencies of peptides $hTERT_{1088}$, $hTERT_{845}$, $hTERT_{167}$, $hTERT_{461}$, $hTERT_{324}$, and $hTERT_{637}$-specific T cells detected by IFN-γ ELISPOT assay and the clinical features of patients. Table 3 shows clinical features of HCC patients who showed positive and negative T cell responses to hTERT-derived epitopes.

The clinical features of both groups were not statistically different in terms of age, sex, serum AFP levels, differentiation of HCC, tumor multiplicity, vascular invasion, TNM factors and stages, histology of the non-tumor liver, liver function, and the type of viral infection (Table 3).

Next, we examined the kinetics of hTERT-specific T cells in 16 patients who had positive T cell responses and received curative treatments by surgical resection or radiofrequent ablation, and analyzed the association between the kinetics and clinical responses. The frequencies of hTERT-specific T cells detected in ELISPOT assay decreased in most of the patients 6 months after curative treatments (Fig. 8). Only 5 of 16 patients showed positive T cell responses after treatments. Four patients whose hTERT-specific T cells were maintained had no recurrence of HCC. In contrast, 11 patients whose number of hTERT-specific T cells decreased showed HCC recurrence within 1 year after curative treatments.

Discussion

In the current study, we first attempted to identify hTERT epitopes restricted by HLA-A24, which is present in 60% of Japanese, 20% of whites, and 12% of Africans,[36,37] using a combined computer-based and immunological approach. Analysis of amino acid sequences of hTERT by computer showed a number of potential HLA-A24–binding peptides, and 2 of the 10 hTERT-derived peptides (Peptides $hTERT_{461}$ and $hTERT_{324}$) have been identified to contain HLA-A24–restricted CTL epitopes. Including these two peptides, six hTERT-derived peptides (peptides $hTERT_{1088}$, $hTERT_{845}$, $hTERT_{167}$, $hTERT_{461}$, $hTERT_{324}$, and $hTERT_{637}$) that showed high affinity for HLA-A*2402 induced production of IFN-γ in spleen cells and PBMCs, in hTERT cDNA-immunized HLA-A*2402/K^b transgenic mice and HCC patients, respectively. In addition, T cell lines stimulated with the peptide showed cytotoxicity against hepatoma cell lines that express HLA-A*2402 and hTERT. Taken together with the results of peptide binding, ELISPOT, and CTL assay, we concluded peptides $hTERT_{1088}$, $hTERT_{845}$, $hTERT_{167}$, $hTERT_{461}$, $hTERT_{324}$, and $hTERT_{637}$ contained HLA-A24 restricted, hTERT-specific CTL epitopes.

Interestingly, the cytotoxicity of hTERT-specific CTLs induced with peptides $hTERT_{1088}$, $hTERT_{845}$, $hTERT_{167}$, and $hTERT_{324}$ in HuH6 cells, which showed low levels of hTERT, was weak compared with the cytotoxicity in HepG2 cells with high levels of hTERT. The difference was even more marked in the cytotoxicity of CTLs induced with peptide $hTERT_{461}$, and the CTLs were not cytotoxic to HuH6. In accordance with our results, it was reported that the susceptibility of tumor cells to hTERT-specific CTLs decreased after IFN-γ

treatment because of attenuation of hTERT expression.[38] In addition, all of the patients who had telomerase activity in the tumor showed hTERT-specific T cell responses in ELISPOT assay. These results suggest that the strength of hTERT-specific cytotoxicity against hepatoma cells depends on the expression levels of the protein.

In the analysis of PBMCs in patients with HCC using $hTERT_{461}$ tetramer, the frequencies of $hTERT_{461}$ tetramer$^+$ cells in PBMCs were similar to those of other tumor specific antigen-derived epitopes.[39] Furthermore, the existence of dysfunctional hTERT-specific T cells was accordant with previous reports of other tumor antigens.[39] Conversely, the frequency of $hTERT_{461}$ tetramer$^+$ cells in tumors was quite high, and they produced IFN-γ. IFN-γ–producing T cells responding to other peptides $hTERT_{1088}$, $hTERT_{845}$, and $hTERT_{167}$ were also detected in tumors. These results suggest that hTERT is an attractive target for immunotherapy of HCC.

In the second part of the current study, to study the status of the host immunological response to hTERT in HCC patients, we examined the frequency of hTERT-specific T cells in the peripheral blood by ELISPOT assay with the six epitopes and analyzed the relationship between the frequency and the clinical features of the patients. ELISPOT assay showed that the frequency of reactive T cells to a single hTERT epitope was 10 to 100 per 3×10^5 PBMCs. In previous reports regarding the frequency of T cells specific for a single hTERT epitope in patients with colon or breast cancer, the number was found to be 1 to 22 per 2×10^5 PBMCs or 1 to 33 per 2×10^5 PBMCs, respectively.[18,19] In addition, single hTERT epitope–specific IFN-γ–producing cells were detected in 6.9% to 12.5% of the patients for peptides $hTERT_{1088}$, $hTERT_{845}$, $hTERT_{167}$, $hTERT_{461}$, $hTERT_{324}$, and $hTERT_{637}$. These rates are quite similar to those in previous reports.[18,19] Comparing the current results with those reports, we believe that hTERT-specific CTL responses in HCC patients are as strong as those of other cancer patients and that the newly identified hTERT epitopes are immunogenic.

From the analysis of hTERT-specific immune responses in HCC patients, we obtained evidence that clinical features, including age, sex, serum AFP levels, differentiation of HCC, tumor multiplicity, vascular invasion, TNM factors and stages, histology of the nontumor liver, liver function, and the type of viral infection, were not associated with the frequency of hTERT-specific CTLs in HCC patients (Table 3). These results suggest that hTERT-specific CTLs could be generated independently of hepatitis viral infection or serum AFP levels, which suppress the host immune response through inhibition of dendritic cells[40-42] or T cell proliferation.[43] In addition, comparing with AFP- or other tumor antigen–specific immune responses,[31,44] hTERT-specific immune responses exist and can be induced in the patients with HCC even at early stages. These results suggest the advantage of hTERT as a target for immunotherapies because the induction of tumor-specific immune responses at early stages of the tumor should be more effective for tumor growth suppression.

In the analysis of the association between kinetics of hTERT-specific T cells and clinical responses, recurrent rate of HCC was higher in the patients without maintenance of hTERT-specific T cells than in those with. This result suggests that maintenance of hTERT-specific T cells may be important to protect tumor recurrence after treatments, although there was no statistically significant difference between the two groups because of the small number of patients.

In conclusion, we identified and characterized HLA-A*2402–restricted T cell epitopes derived from hTERT. The identified epitope-specific T cells can be detected and induced by stimulating PBMCs with these peptides in HCC patients. hTERT-specific CTLs were observed even in the patients with early stages of HCC and killed hepatoma cell lines that expressed hTERT dependent on the expression level. The frequency of hTERT/tetramer$^+$CD8$^+$ T cells in the tumor tissue of patients with HCC was quite high, and they were functional. These results suggest that hTERT is an important target of T-cell–based immunotherapy for HCC and that the identified epitopes could be valuable both for therapy and for analyzing the host immune responses.

Acknowledgment: The authors thank Maki Kawamura, Sanae Funaoka, and Chiharu Minami for their invaluable help with sample collection, and all patients who donated blood samples for this study.

References

1. Parkin DM, Bray F, Ferlay J, Pisani P. Estimating the world cancer burden: Globocan 2000. Int J Cancer 2001;94:153-156.
2. El-Serag HB, Mason AC. Rising incidence of hepatocellular carcinoma in the United States. N Engl J Med 1999;340:745-750.
3. Deuffic S, Poynard T, Buffat L, Valleron AJ. Trends in primary liver cancer. Lancet 1998;351:214-215.
4. Curley SA, Izzo F, Ellis LM, Nicolas Vauthey J, Vallone P. Radiofrequency ablation of hepatocellular cancer in 110 patients with cirrhosis. Ann Surg 2000;232:381-391.
5. Urabe T, Kaneko S, Matsushita E, Unoura M, Kobayashi K. Clinical pilot study of intrahepatic arterial chemotherapy with methotrexate, 5-fluorouracil, cisplatin and subcutaneous interferon-alpha-2b for patients with locally advanced hepatocellular carcinoma. Oncology 1998;55:39-47.
6. Mazzaferro V, Regalia E, Doci R, Andreola S, Pulvirenti A, Bozzetti F, et al. Liver transplantation for the treatment of small hepatocellular carcinomas in patients with cirrhosis. N Engl J Med 1996;334:693-699.
7. Meyerson M, Counter CM, Eaton EN, Ellisen LW, Steiner P, Caddle SD, et al. hEST2, the putative human telomerase catalytic subunit gene, is up-regulated in tumor cells and during immortalization. Cell 1997;90:785-795.

8. Nakamura TM, Morin GB, Chapman KB, Weinrich SL, Andrews WH, Lingner J, et al. Telomerase catalytic subunit homologs from fission yeast and human. Science 1997;277:955-959.
9. Nakayama J, Tahara H, Tahara E, Saito M, Ito K, Nakamura H, et al. Telomerase activation by hTRT in human normal fibroblasts and hepatocellular carcinomas. Nat Genet 1998;18:65-68.
10. Harrington L, Zhou W, McPhail T, Oulton R, Yeung DS, Mar V, et al. Human telomerase contains evolutionarily conserved catalytic and structural subunits. Genes Dev 1997;11:3109-3115.
11. Vonderheide RH, Hahn WC, Schultze JL, Nadler LM. The telomerase catalytic subunit is a widely expressed tumor-associated antigen recognized by cytotoxic T lymphocytes. Immunity 1999;10:673-679.
12. Vonderheide RH, Anderson KS, Hahn WC, Butler MO, Schultze JL, Nadler LM. Characterization of HLA-A3-restricted cytotoxic T lymphocytes reactive against the widely expressed tumor antigen telomerase. Clin Cancer Res 2001;7:3343-3348.
13. Scardino A, Gross DA, Alves P, Schultze JL, Graff-Dubois S, Faure O, et al. HER-2/neu and hTERT cryptic epitopes as novel targets for broad spectrum tumor immunotherapy. J Immunol 2002;168:5900-5906.
14. Saeboe-Larssen S, Fossberg E, Gaudernack G. mRNA-based electrotransfection of human dendritic cells and induction of cytotoxic T lymphocyte responses against the telomerase catalytic subunit (hTERT). J Immunol Methods 2002;259:191-203.
15. Frolkis M, Fischer MB, Wang Z, Lebkowski JS, Chiu CP, Majumdar AS. Dendritic cells reconstituted with human telomerase gene induce potent cytotoxic T-cell response against different types of tumors. Cancer Gene Ther 2003;10:239-249.
16. Parkhurst MR, Riley JP, Igarashi T, Li Y, Robbins PF, Rosenberg SA. Immunization of patients with the hTERT:540-548 peptide induces peptide-reactive T lymphocytes that do not recognize tumors endogenously expressing telomerase. Clin Cancer Res 2004;10:4688-4698.
17. Verra NC, Jorritsma A, Weijer K, Ruizendaal JJ, Voordouw A, Weder P, et al. Human telomerase reverse transcriptase-transduced human cytotoxic T cells suppress the growth of human melanoma in immunodeficient mice. Cancer Res 2004;64:2153-2161.
18. Amarnath SM, Dyer CE, Ramesh A, Iwuagwu O, Drew PJ, Greenman J. In vitro quantification of the cytotoxic T lymphocyte response against human telomerase reverse transcriptase in breast cancer. Int J Oncol 2004; 25:211-217.
19. Titu LV, Loveday RL, Madden LA, Cawkwell L, Monson JR, Greenman J. Cytotoxic T-cell immunity against telomerase reverse transcriptase in colorectal cancer patients. Oncol Rep 2004;12:871-876.
20. Schreurs MW, Kueter EW, Scholten KB, Kramer D, Meijer CJ, Hooijberg E. Identification of a potential human telomerase reverse transcriptase-derived, HLA-A1-restricted cytotoxic T-lymphocyte epitope. Cancer Immunol Immunother 2005;54:703-712.
21. Araki T, Itai Y, Furui S, Tasaka A. Dynamic CT densitometry of hepatic tumors. AJR Am J Roentgenol 1980;135:1037-1043.
22. Japan. LCSGo. Classification of Primary Liver Cancer. English ed 2. Tokyo:Kanehara & Co.,Ltd. 1997.
23. Desmet VJ, Gerber M, Hoofnagle JH, Manns M, Scheuer PJ. Classification of chronic hepatitis: diagnosis, grading and staging. HEPATOLOGY 1994;19:1513-1520.
24. Ikeda-Moore Y, Tomiyama H, Miwa K, Oka S, Iwamoto A, Kaneko Y, et al. Identification and characterization of multiple HLA-A24-restricted HIV-1 CTL epitopes: strong epitopes are derived from V regions of HIV-1. J Immunol 1997;159:6242-6252.
25. Kuzushima K, Hayashi N, Kimura H, Tsurumi T. Efficient identification of HLA-A*2402-restricted cytomegalovirus-specific CD8(+) T-cell epitopes by a computer algorithm and an enzyme-linked immunospot assay. Blood 2001;98:1872-1881.
26. Butterfield LH, Meng WS, Koh A, Vollmer CM, Ribas A, Dissette VB, et al. T cell responses to HLA-A*0201-restricted peptides derived from human alpha fetoprotein. J Immunol 2001;166:5300-5308.
27. Oiso M, Eura M, Katsura F, Takiguchi M, Sobao Y, Masuyama K, et al. A newly identified MAGE-3-derived epitope recognized by HLA-A24-restricted cytotoxic T lymphocytes. Int J Cancer 1999;81:387-394.
28. Arai K, Masutomi K, Khurts S, Kaneko S, Kobayashi K, Murakami S. Two independent regions of human telomerase reverse transcriptase are important for its oligomerization and telomerase activity. J Biol Chem 2002;277: 8538-8544.
29. Gotoh M, Takasu H, Harada K, Yamaoka T. Development of HLA-A2402/K(b) transgenic mice. Int J Cancer 2002;100:565-570.
30. Mizukoshi E, Nascimbeni M, Blaustein JB, Mihalik K, Rice CM, Liang TJ, et al. Molecular and immunological significance of chimpanzee major histocompatibility complex haplotypes for hepatitis C virus immune response and vaccination studies. J Virol 2002;76:6093-6103.
31. Mizukoshi E, Nakamoto Y, Tsuji H, Yamashita T, Kaneko S. Identification of alpha-fetoprotein-derived peptides recognized by cytotoxic T lymphocytes in HLA-A24+ patients with hepatocellular carcinoma. Int J Cancer 2006;118:1194-204.
32. Wedemeyer H, Mizukoshi E, Davis AR, Bennink JR, Rehermann B. Cross-reactivity between hepatitis C virus and Influenza A virus determinant-specific cytotoxic T cells. J Virol 2001;75:11392-11400.
33. Nakamoto Y, Kaneko S, Takizawa H, Kikumoto Y, Takano M, Himeda Y, et al. Analysis of the CD8-positive T cell response in Japanese patients with chronic hepatitis C using HLA-A*2402 peptide tetramers. J Med Virol 2003;70:51-61.
34. Sobin LH WC. TNM Classification of Malignant Tumors, 6th ed. New York: Wiley-Liss 2002:81.
35. Arai J, Yasukawa M, Ohminami H, Kakimoto M, Hasegawa A, Fujita S. Identification of human telomerase reverse transcriptase-derived peptides that induce HLA-A24-restricted antileukemia cytotoxic T lymphocytes. Blood 2001;97:2903-2907.
36. Imanishi T, Akaza, T, Kimura A, Tokunaga K, Gojobori T. Allele and Haplotype Frequencies for HLA and Complement Loci in Various Ethnic Groups. Oxford Scientific Publications, Oxford 1992:1065-1220.
37. Tokunaga K, Ishikawa Y, Ogawa A, Wang H, Mitsunaga S, Moriyama S, et al. Sequence-based association analysis of HLA class I and II alleles in Japanese supports conservation of common haplotypes. Immunogenetics 1997;46:199-205.
38. Tajima K, Ito Y, Demachi A, Nishida K, Akatsuka Y, Tsujimura K, et al. Interferon-gamma differentially regulates susceptibility of lung cancer cells to telomerase-specific cytotoxic T lymphocytes. Int J Cancer 2004;110: 403-412.
39. Shang XY, Chen HS, Zhang HG, Pang XW, Qiao H, Peng JR, et al. The spontaneous CD8+ T-cell response to HLA-A2-restricted NY-ESO-1b peptide in hepatocellular carcinoma patients. Clin Cancer Res 2004;10: 6946-6955.
40. Kanto T, Hayashi N, Takehara T, Tatsumi T, Kuzushita N, Ito A, et al. Impaired allostimulatory capacity of peripheral blood dendritic cells recovered from hepatitis C virus-infected individuals. J Immunol 1999;162: 5584-5591.
41. Auffermann-Gretzinger S, Keeffe EB, Levy S. Impaired dendritic cell maturation in patients with chronic, but not resolved, hepatitis C virus infection. Blood 2001;97:3171-3176.
42. Beckebaum S, Cicinnati VR, Zhang X, Ferencik S, Frilling A, Grosse-Wilde H, et al. Hepatitis B virus-induced defect of monocyte-derived dendritic cells leads to impaired T helper type 1 response in vitro: mechanisms for viral immune escape. Immunology 2003;109:487-495.
43. Peck AB, Murgita RA, Wigzell H. Cellular and genetic restrictions in the immunoregulatory activity of alpha-fetoprotein. II. Alpha-fetoprotein-induced suppression of cytotoxic T lymphocyte development. J Exp Med 1978;148:360-372.
44. Nagorsen D, Keilholz U, Rivoltini L, Schmittel A, Letsch A, Asemissen AM, et al. Natural T-cell response against MHC class I epitopes of epithelial cell adhesion molecule, her-2/neu, and carcinoembryonic antigen in patients with colorectal cancer. Cancer Res 2000;60:4850-4854.

JOURNAL OF VIROLOGY, Apr. 2006, p. 3332–3340
0022-538X/06/$08.00+0 doi:10.1128/JVI.80.7.3332–3340.2006

Vol. 80, No. 7

Effect of Hepatitis C Virus (HCV) NS5B-Nucleolin Interaction on HCV Replication with HCV Subgenomic Replicon

Tetsuro Shimakami,[1] Masao Honda,[1] Takashi Kusakawa,[2] Takayuki Murata,[3] Kunitada Shimotohno,[3] Shuichi Kaneko,[1] and Seishi Murakami[2]*

Department of Gastroenterology, Kanazawa University Graduate School of Medicine,[1] and Department of Molecular Oncology, Cancer Research Institute, Kanazawa University,[2] Takara-Machi, Kanazawa, Ishikawa 920-0934, and Department of Viral Oncology, Institute for Virus Research, Kyoto University, Kawara-Cho, Sakyo-Ku, Kyoto 606-8507,[3] Japan

Received 25 September 2005/Accepted 5 January 2006

We previously reported that nucleolin, a representative nucleolar marker, interacts with nonstructural protein 5B (NS5B) of hepatitis C virus (HCV) through two independent regions of NS5B, amino acids 208 to 214 and 500 to 506. We also showed that truncated nucleolin that harbors the NS5B-binding region inhibited the RNA-dependent RNA polymerase activity of NS5B in vitro, suggesting that nucleolin may be involved in HCV replication. To address this question, we focused on NS5B amino acids 208 to 214. We constructed one alanine-substituted clustered mutant (CM) replicon, in which all the amino acids in this region were changed to alanine, as well as seven different point mutant (PM) replicons, each of which harbored an alanine substitution at one of the amino acids in the region. After transfection into Huh7 cells, the CM replicon and the PM replicon containing NS5B W208A could not replicate, whereas the remaining PM replicons were able to replicate. In vivo immunoprecipitation also showed that the W208 residue of NS5B was essential for its interaction with nucleolin, strongly suggesting that this interaction is essential for HCV replication. To gain further insight into the role of nucleolin in HCV replication, we utilized the small interfering RNA (siRNA) technique to investigate the knockdown effect of nucleolin on HCV replication. Cotransfection of replicon RNA and nucleolin siRNA into Huh7 cells moderately inhibited HCV replication, although suppression of nucleolin did not affect cell proliferation. Taken together, our findings strongly suggest that nucleolin is a host component that interacts with HCV NS5B and is indispensable for HCV replication.

Hepatitis C virus (HCV) is a major cause of chronic hepatitis around the world (1, 7). Chronic infection with HCV results in liver cirrhosis and may lead to hepatocellular carcinoma (53, 54). HCV is an enveloped positive-strand RNA virus belonging to the genus *Hepacivirus* in the family *Flaviviridae*. The HCV RNA genome is ~9.6 kb in length and consists of a 5′ nontranslated region (NTR), a large open reading frame, and a 3′ NTR. The 5′ NTR contains an internal ribosome entry site, which mediates the translation of a single polyprotein of ~3,000 amino acid (aa) residues (61, 64). This polyprotein is cleaved by host and viral proteases into at least 10 different products (33). At the amino terminus of the polyprotein are the core protein, E1, and E2, followed by p7, a hydrophobic peptide with unknown function, and the nonstructural (NS) proteins NS2, NS3, NS4A, NS4B, NS5A, and NS5B. The 3′ NTR consists of a short variable sequence, a poly(U)-poly(UC) tract, and a highly conserved X region and is critical for HCV RNA replication and HCV infection (13, 29, 69, 71).

HCV is unique among positive-strand RNA viruses in that it causes persistent and chronic infections. In addition, the high mutation rate of the gene encoding the E2 protein allows it to escape host immune surveillance, which is strongly associated with chronic inflammation of the liver (19, 23, 66, 67). As a result, HCV replication has become a target for the treatment of chronically infected individuals. The RNA-dependent RNA polymerase (RdRp) NS5B is the central catalytic enzyme in HCV RNA replication. Several recombinant and catalytically active forms of NS5B have been expressed and purified from insect cells and *Escherichia coli*, and these proteins have provided insights into the biochemical and catalytic properties of NS5B (2, 12, 34, 68). Studies of HCV replication in vitro have to overcome several difficulties, since replication requires all or most NS proteins and/or host proteins and occurs at the membrane. An understanding of the biology of HCV replication has been facilitated by the development of subgenomic and full-length HCV replicons, which express HCV proteins and replicate their RNA when transfected into human hepatoma-cell-derived Huh7 cells and other cell lines (22, 24, 35).

Nucleolin is a major nucleolar phosphoprotein, and nucleolin-specific antibodies have been used to identify nucleoli (14, 59). Nucleolin has been shown to be an RNA chaperone and/or shuttling protein for various host and viral components in nucleoli, nucleoplasm, cytoplasm, and the plasma membrane (18, 37, 41). We previously reported that the transient expression of NS5B causes the redistribution of endogenous nucleolin from the nucleus to the cytoplasm and that nucleolin and NS5B interact, in vitro and in vivo, through two independent regions of NS5B, aa 208 to 214 and 500 to 506. We also showed that the C-terminal region of nucleolin inhibited NS5B RdRp activity through this interaction in vitro (20). Because full-length nucleolin was not available in that experimental condition (70), we could not determine the exact role of this interaction in vivo.

To further investigate the interaction between nucleolin and NS5B, we focused on NS5B aa 208 to 214. We prepared a

* Corresponding author. Mailing address: Department of Molecular Oncology, Cancer Research Institute, Kanazawa University, 13-1 Takara-Machi, Kanazawa, Ishikawa, Japan. Phone: 81-76-265-2731. Fax: 81-76-234-4501. E-mail: semuraka@kenroku.kanazawa-u.ac.jp.

series of mutant replicons in which each amino acid within this region was altered to alanine(s). Here, we report that the W208 residue is critical for transient HCV replication as well as for binding to nucleolin in vivo. HCV replication was considerably inhibited in cells in which endogenous nucleolin was transiently down-regulated by small interfering RNA (siRNA). Our results strongly suggest the involvement of nucleolin in HCV replication through its interaction with NS5B and that nucleolin acts as a positive modulator of HCV replication.

MATERIALS AND METHODS

Construction of plasmids. The plasmid pNNRZ2RU (28), which harbors a subgenomic replicon derived from MT-2C cells infected with HCV (a genotype 1b isolate, M1LE [GenBank accession no. AB080299]) and contains wild-type M1LE replicon (M1LE/wild) cDNA, was digested with MluI and BglII, and the obtained fragment was inserted into the MluI and BglII sites of the vector pGL3Basic (Promega) to create pGL3-*MluI-BglII*. The intermediate vector pGL3-*MluI-BglII*-S2321 was constructed by introducing the point mutation S2321 of NS5A into the MluI and SacI sites of pGL3-*MluI-BglII* by site-directed mutagenesis using primers carrying the necessary nucleotide changes. Subsequently, mutations were introduced into pGL3-*MluI-BglII*-S2321, which was digested with MluI and BglII. The resulting DNA fragments were subsequently ligated into the MluI and BglII sites of pNNRZ2RU. Plasmids containing the individual NS5B substitutions W208A, K209A, S210A, K211A, K212A, C213A, and P214A and the 7-amino-acid alanine substitution, cm211, were constructed by introducing each mutation into the Eco81I and NdeI sites of pGL3-*MluI-BglII*-S2321 by site-directed mutagenesis using primers carrying the necessary nucleotide changes.

The vector pNKFLAG (49) was used to express amino-terminally FLAG-tagged proteins. The plasmid pNNRZ2RU was subcloned by PCR using the primers 5′-TATCGAGCTCGATGTCAATGTCCTACTCATGGACAGGT-3′ (NS5B For), which contains an artificial initiation codon downstream of the SacI site, and 5′-ATGGATGGATCCGCGGGGTCGGGCGCGAGACAGGCT-3′ (NS5Bt Rev), which contains a BamHI site. NS5Bt, containing full-length NS5B truncated by 21 aa at the C terminus, was subcloned into the SacI and BamHI sites of pNKFLAG to create pNKFLAGNS5Bt.

The plasmid pNKGST/Nucleolin (20) was used for the expression of glutathione-*S*-transferase (GST)-fused nucleolin proteins. FLAG-labeled plasmids containing the individual NS5B substitutions W208A, K209A, S210A, K211A, K212A, C213A, and P214A and the 7-amino-acid alanine substitution cm211 were constructed by introducing fragments of pGL3-*MluI-BglII*-S2321 containing each mutation into the EcoRI and SmaI sites of pNKFLAGNS5Bt.

The sequences of all the constructs were confirmed using the dideoxy sequence method. The plasmids pLMH14 and pLMH14/GHD (40) were used as templates for replicon RNA LMH14 and LMH14/GHD, respectively.

Cell culture. We used two kinds of Huh7 cells, one derived from our own laboratory's original Huh7 cells, designated Huh7-DMB (56), and the other cured of MH14 gamma interferon, designated cured MH14 (40). Huh7-DMB cells were used for colony-forming assays, and cured MH14 cells were used for luciferase assays. Both types of Huh7 cells were grown in Dulbecco's modified Eagle's medium (Gibco-BRL, Invitrogen Life Technologies) supplemented with 10% fetal bovine serum, 2 mM L-glutamine, nonessential amino acids, 100 U of penicillin, and 100 μg of streptomycin.

In vitro transcription and purification of RNA. All plasmids harboring replicon RNA were linearized with XbaI and column purified (PCR purification kit; Promega). RNA was synthesized and purified as described previously (56).

RNA transfection and selection of G418-resistant cells. Subconfluent Huh7 cells were trypsinized, washed once with phosphate-buffered saline (PBS) that does not contain Ca and Mg [PBS(−)], and resuspended at 10^7 cells/ml in OPTI-MEM (Gibco-BRL, Invitrogen Life Technologies). One hundred nanograms of *neo* replicon RNA, with or without 1 μM of each siRNA, was added to 400 μl of each cell suspension in a cuvette with a gap width of 0.4 cm (Bio-Rad). The mixture was immediately transfected into Huh7 cells by electroporation with a GenePulser II system (Bio-Rad) set to 270 V and 975 μF. Following a 10-min incubation at room temperature, the cells were transferred into 10 ml of growth medium and seeded into a 10-cm-diameter cell culture dish. To select G418-resistant cells, the medium was replaced with fresh medium containing 1 mg/ml of G418 (GENETICIN; Gibco-BRL, Invitrogen Life Technologies) 24 h after transfection. After changing the medium twice per week for 4 weeks, the colonies were stained with Coomassie brilliant blue (0.6 g/liter in 50% methanol–10% acetic acid).

DNA transfection. Using the same electroporation protocol as described above, 500 ng of pCI-Neo (Promega), which encodes a neomycin resistance marker under the control of a cytomegalovirus (CMV) promoter/enhancer, with or without 1 μM of each siRNA, was transfected into Huh7 cells. G418-resistant cells were selected in medium containing 0.5 mg/ml G418. Four weeks after transfection, the colonies were stained with Coomassie brilliant blue.

Using DMRIE-C reagent (Invitrogen Life Technologies), 300 ng of pGL3 control (Promega), encoding luciferase under the control of a CMV promoter/enhancer, was cotransfected with or without 2 μM of each siRNA according to the manufacturer's instructions. Luciferase activity was assayed 48 and 72 h after transfection.

RNA transfection and luciferase assay. We used a luciferase assay to monitor luciferase replicon activity. Briefly, cured MH14 cells seeded onto 48-well plates were transfected with 250 ng of luciferase replicon RNA, with or without 2 μM of each siRNA, using DMRIE-C reagent according to the manufacturer's instructions. Cell proteins were extracted in a lysis buffer supplied in the Dual-Luciferase Reporter Assay system (Promega), and their luciferase activity was measured. Each assay was performed at least in triplicate, and means and standard deviations were determined.

Preparation of cell extracts, coprecipitation with glutathione resin, and Western blot analysis. COS1 cells were transiently transfected using the calcium-phosphate method. The cells were harvested, washed with PBS(−), and sonicated in PBS lysis buffer [PBS(−) containing 150 mM NaCl, 1.0% Triton X-100, 1 mM EDTA, and 1 mM dithiothreitol] containing 10 μg each of aprotinin and leupeptin per ml. Total cell lysates were diluted 10-fold with PBS lysis buffer, mixed with 20 μl of glutathione-Sepharose 4B beads (glutathione resin) (Amersham Biosciences), and incubated for 3 h on a rotator in a cold room. After extensive washing with PBS(−) containing 1.0% Triton X-100, the bound proteins were eluted, fractionated by sodium dodecyl sulfate (SDS)–10% polyacrylamide gel electrophoresis (PAGE), transferred onto nitrocellulose membranes, and subjected to Western blot analysis with anti-FLAG M2 monoclonal antibody (Sigma). The proteins were visualized using enhanced chemiluminescence according to the manufacturer's instructions (Amersham Biosciences). As a loading control, the nitrocellulose membranes used for Western blot analysis with anti-FLAG M2 monoclonal antibody were reprobed with anti-GST monoclonal antibody (Santa Cruz Biotechnology, Inc.) according to the manufacturer's instructions (Amersham Biosciences).

siRNA. We purchased siRNA for luciferase GL3 duplex (si-Luc), siRNA for nonspecific control RNA duplex (si-Mix), siRNA for nucleolin (si-Nuc) (GGA AGACGGUGAAAUUGAU-deoxyribosylthymine [dT]dT), and siRNA for HCV (CCUCAAAGAAAAACCAAAC-dTdT) from B-Bridge International, Inc., and we purchased siRNA for GFP from QIAGEN.

Western blot analysis for endogenous nucleolin. Using the electroporation protocol described above, 1 μM of each siRNA was transfected into Huh7-DMB cells. After 48 h, the cells were harvested, washed with PBS(−), and sonicated in PBS lysis buffer. Total cell lysates were fractionated by SDS–10% PAGE, transferred onto nitrocellulose membranes, and subjected to Western blot analysis with rabbit polyclonal anti-nucleolin antibody (103C) (20), mouse monoclonal anti-nucleolin antibody (C23, sc-8031; Santa Cruz Biotechnology, Inc.), and mouse monoclonal anti-β-actin antibody (Sigma). The proteins were visualized by enhanced chemiluminescence according to the manufacturer's instructions (Amersham Biosciences).

RESULTS

We previously reported that NS5B from HCV subtype 1b isolate JK-1 and nucleolin interact in vitro and in vivo and that two regions of NS5B, amino acids 208 to 214 and 500 to 506, are both indispensable for binding to nucleolin. We also reported that the C-terminal region of nucleolin inhibited the RdRp activity of NS5B in a dose-dependent manner (20). Although the effect of full-length nucleolin could not be determined, because we could not obtain recombinant full-length nucleolin, these results strongly suggested that nucleolin may be a component of the HCV replication complex and, through its interaction with NS5B, may modulate HCV replication. To further investigate this question, we determined the biological effect of the interaction between NS5B from HCV subtype 1b

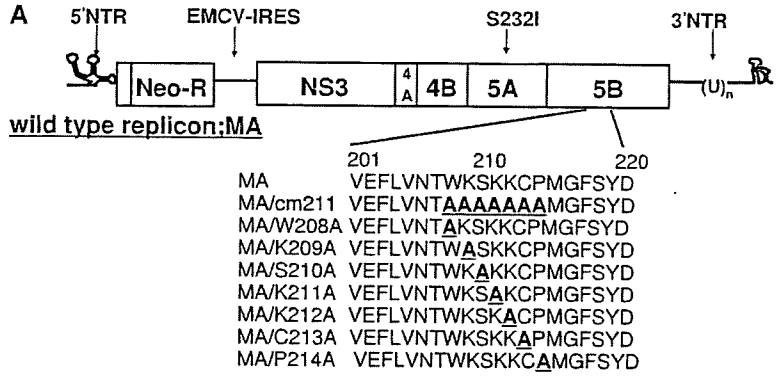

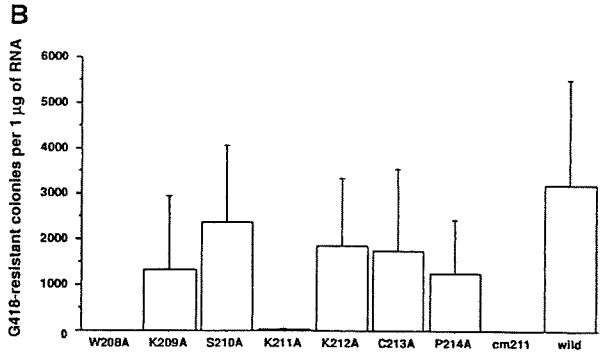

FIG. 1. (A) Schematic representation of the mutant replicons used in this study. MA is a replicon carrying the point mutation S232I in NS5A and was used as the wild-type replicon. The mutant replicons MA/cm211, MA/W208A, MA/209A, MA/S210A, MA/211A, MA/212A, MA/213A, and MA/214A carry NS5B mutations in MA, as shown. Numbering starts from the beginning of NS5B. EMCV, encephalomyocarditis virus; IRES, internal ribosome entry site. (B) Effect of each mutation on HCV RNA replication. Huh7-DMB cells were electroporated with 1 μg of each replicon RNA, and G418-resistant cells were selected with 1 mg/ml G418 and stained 4 weeks later. This figure shows the mean number of G418-resistant cell colonies per 10-cm-diameter cell culture dish per 1 μg replicon RNA.

isolate M1LE and nucleolin on HCV replication using an HCV subgenomic replicon system.

Scanning of aa 208 to 214 in an HCV subgenomic replicon. First, we tested the importance of NS5B aa 208 to 214, a region essential for nucleolin binding, in HCV RNA replication. For this purpose, we prepared eight mutant replicons (Fig. 1A). The wild-type replicon was represented by MA, in which S232 of NS5A was altered to I, because this mutant replicon can efficiently replicate in Huh7 cells (36, 56). In the replicon MA/cm211, each of the amino acids at positions 208 to 214 of NS5B was changed to alanine, whereas in the replicons MA/W208A, K209A, S210A, K211A, K212A, C213A, and P214A, each individual amino acid residue was changed to alanine. All of these mutant replicons were transfected into Huh7-DMB cells, which were selected with G418, and the number of G418-resistant colonies was used as an indication of HCV RNA replication. In cells transfected with MA/cm211 and MA/W208A, we observed no G418-resistant colonies, whereas in cells transfected with the six other point mutant replicons, as well as in cells transfected with MA/K211, we detected G418-resistant colonies, but they were fewer than those detected with wild-type replicon MA (Fig. 1B). Our negative control, the mutant replicon M1LE/5B-VDD, in which the GDD motif of NS5B was mutated to VDD, yielded no G418-resistant colonies (data not shown). The results of this experiment indicated that the region of NS5B at aa 208 to 214, especially W208, is essential for HCV RNA replication.

Interaction between nucleolin and NS5B. Although we have shown that NS5B from isolate JK-1 binds to nucleolin, it was necessary to show this in isolate M1LE. Due to the poor recovery of soluble full-length NS5B, we utilized NS5Bt (68), a soluble form of NS5B in which the C-terminal 21 aa were truncated, to dissect the interaction between NS5B and nucleolin. Previously, we confirmed that these 21 deleted amino acids were not essential for this interaction (20). FLAG-NS5Bt and GST-nucleolin were transiently coexpressed in COS1 cells, after which the lysates were subjected to a GST pull-down assay and the bound proteins were immunologically detected with anti-FLAG M2 and anti-GST antibodies. We found that GST-nucleolin could bind FLAG-NS5Bt from the M1LE isolate, whereas GST could not, indicating that nucleolin interacts with NS5B in both JK-1 and M1LE isolates (Fig. 2). To determine the essential region/residues of NS5B required for its binding to nucleolin, we again focused on aa 208 to 214 using the alanine scanning method (3). We prepared FLAG-NS5Bt/cm211, in which aa 208 to 214 were all replaced by alanine residues, and showed that it could not bind to GST-nucleolin in an in vivo immunoprecipitation assay (Fig. 2), indicating that aa 208 to 214 of NS5B in both M1LE and JK-1 isolates constitute a critical region for the binding of nucleolin. To identify the exact residue(s) within aa 208 to 214 critical for binding to nucleolin, we prepared seven alanine-substituted point mutants in which each amino acid was replaced by alanine, and we tested the ability of each point mutant to bind to GST-nucleolin. Using an in vivo immunoprecipitation assay, we found that of the seven point mutants, only FLAG-NS5Bt/W208A could not bind to GST-nucleolin (Fig. 2), indicating that W208 of NS5B is essential for this binding and may be essential for HCV replication.

Suppression of endogenous nucleolin by siRNA. To identify the siRNA sequence that knocks down the expression of endogenous nucleolin, we used the prediction services of